

Synthesis of Fluorinated Oligomers toward Physical Vapor Deposition Molecular Electronics Candidates

Francisco Maya, Stéphanie H. Chanteau, Long Cheng, Michael P. Stewart, and James M. Tour*

Department of Chemistry and Center for Nanoscale Science and Technology, MS 222, Rice University, 6100 Main Street, Houston, Texas 77005

Received August 18, 2004. Revised Manuscript Received December 20, 2004

New electron-deficient fluorinated oligo(phenylene ethynylenes) (OPEs) with varied functional groups were synthesized as free thiols, nitriles, and pyridines, ready to be used for surface adhesion. Calculated dipole moments suggest better matching between energy levels of bulk interfaces and molecular frontier orbitals when compared to nonfluorinated OPEs. Differential scanning calorimetry confirmed a higher thermal stability than the nonfluorinated counterparts. Surface analysis by ellipsometry, contact angle goniometry, cyclic voltammetry, and surface infrared and X-ray photoelectron spectroscopy verified that the OPEs chemisorb on Au and Pt surfaces. On the basis of the physical properties of the fluorinated OPEs, they might be useful in future physical vapor deposition techniques, methods that are typically used in standard semiconductor fabrication processes.

1. Introduction

The development of electronic devices based on conjugated organic molecules has been one of the “bottom-up” approaches developed to address the present physical and economic limitations that arise as integrated circuits are miniaturized.¹ Through this approach, we have been pursuing molecular diversity by the rational design of linear conjugated oligomers that possess not only the conductive characteristics similar to those of previous molecular devices,² but also address specific challenges presented in the fabrication process of these electronic devices. To that end, we report here the synthesis of new oligo(phenylene ethynylene) (OPE) derivatives with a range of surface bonding moieties (alligator clips) and functional groups, including an electron-deficient polyfluoroarene. The objective with these new OPEs is to alter the thermal, chemical, and electronic properties of the molecules, to make them suitable for integration with solid-state devices. Such alterations may offer new benefits to electronic devices based on present fabrication approaches.

In general, the use of fluorocarbons as organic thin film precursors produces materials with increased thermal stability and chemical resistance. The intermolecular attractive forces become less dominant so that the molecular interactions at the chemical interface level become more pronounced compared to those of the nonfluorinated analogues.³ This is especially true for aromatic fluorine compounds.⁴ These

characteristics could be critical for high-temperature processes such as gas-phase physical vapor deposition (PVD).⁵ PVD at ultrahigh vacuum (UHV) has been pursued as an alternative to solution-phase formation of self-assembled monolayers (SAMs),⁶ and specifically as a method for the production of molecular electronic devices. For these electronic architectures that are assembled using PVD, the integrity and thermal stability of the organic layers are critical. This has been the case for pentafluorophenyl comonomers⁷ and vinyl monomers,⁸ among other oligomers,^{9,10} that have been used as candidates for dielectric and optical waveguide devices due their improved electronic properties.¹¹

With the goal of producing several new molecular electronics candidates that would be appropriate for PVD applications, we present the synthesis of nine oligomers shown in Figure 1. The central core of these oligomers has been functionalized with nitro or amine groups, which have been widely reported to act as redox centers for switching effects.²

The OPEs were functionalized with various alligator clips, including free thiols,^{12,13} nitriles,¹⁴ and pyridines^{15,16} for

- * To whom correspondence should be addressed. E-mail: tour@rice.edu.
- (1) Tour, J. M. *Molecular Electronics: Commercial Insights, Chemistry, Devices, Architecture and Programming*; World Scientific: River Edge, NJ, 2003.
 - (2) Chen, J.; Wang, J.; Reed, M. A.; Rawlett, A. M.; Price, D. W.; Tour, J. M. *Appl. Phys. Lett.* **2000**, *77*, 1224.
 - (3) Olah, G. A. *Fluorine in Organic Chemistry, Interscience Monographs on Organic Chemistry*; John Wiley & Sons: New York, 1973.
 - (4) Pavlath, A. E.; Leffler, A. J. *Aromatic Fluorine Compounds*; Reinhold Publishing Corporation: New York, 1962.

- (5) Chiang, L. Y.; Swirczewski, J. W.; Lai, F.; Goshorn, D. P. *Synth. Met.* **1991**, *41*, 1425.
- (6) Song, W. J.; Seoul, C.; Kang, G.-W.; Lee, C. *Synth. Met.* **2000**, *41*, 1425.
- (7) Pitois, C.; Vukmirovic, S.; Hulst, A.; Wiesmann, D.; Robertsson, M. *Macromolecules* **1999**, *32*, 2903.
- (8) Kim, J. P.; Lee, W. Y.; Kang, J. W.; Kwon, S. K.; Kim, J. J.; Lee, J. S. *Macromolecules* **2001**, *34*, 7817.
- (9) Elada, L. A.; Shacklette, L. W.; Norwood, R. A.; Yardley, J. T. *SPIE Crit. Rev.* **1997**, *CR68*, 207.
- (10) Kobayashi, J.; Matsuura, T.; Hida, Y.; Sasaki, S.; Maruno, T. *J. Lightwave Technol.* **1998**, *16*, 1024.
- (11) Wang, J.; Sustack, P.; Garner, S. *Proc. SPIE* **2002**, *129*, 4904.
- (12) Dhirani, A.; Lin, P.-H.; Guyot-Sionnest, P.; Zehner, R. W.; Sita, L. R. *J. Chem. Phys.* **1997**, *196*, 5249.
- (13) Cygan, M. T.; Dunbar, T. D.; Arnold, J. J.; Bumm, L. A.; Shedlock, N. F. *J. Am. Chem. Soc.* **1998**, *120*, 2721.

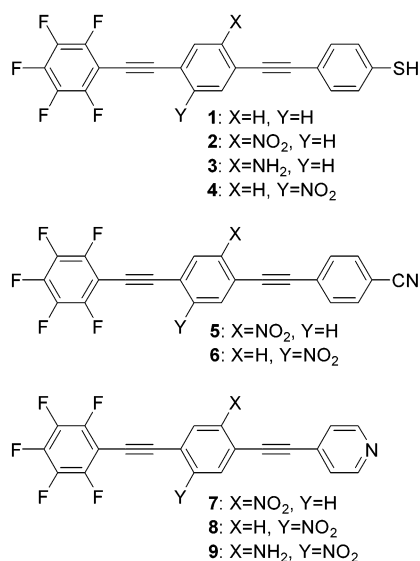


Figure 1. Fluorinated OPEs reported in this work.

66 making molecular scale junctions with several bulk con-
 67 tacts.¹⁷ Each new molecule contained an electron-deficient
 68 pentafluoro aromatic ring as the dipole moment director.
 69 Thermal analyses on these new oligomers were performed
 70 by differential scanning calorimetry (DSC) to gain insights
 71 into their thermal stability and their possible use in PVD
 72 processes. Theoretical values of their dipole moments and
 73 frontier orbital energies were calculated using density
 74 functional theory as explained in the Experimental Section.

75 Surface analysis of chemisorbed compounds on Au and
 76 Pt was performed by ellipsometry, contact angle goniometry,
 77 Fourier transform infrared (FTIR) analysis, and X-ray
 78 photoelectron spectroscopy (XPS).

2. Results

80 **2.1. Theoretical Calculations.** For conjugated linear
 81 molecules, it has been demonstrated that better control and
 82 improvement of electronic charge and hole injection is
 83 possible when utilizing fluorinated OPEs.¹⁸ Because of the
 84 lower intermolecular interaction, OPEs with fluorine sub-
 85 stituents also demonstrated tighter molecular packing in
 86 SAMs¹⁹ and behaved as *n*-type organic semiconductors.²⁰
 87 As reported by Campbell and co-workers,²¹ such electronic
 88 effects were possible by manipulating the Schottky energy
 89 barrier, which is the energy gap between the work function
 90 of the bulk interface and the molecular frontier orbitals. A
 91 high dipole moment driven by the electron-deficient fluori-

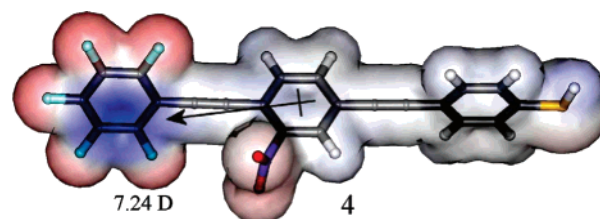


Figure 2. Electrostatic surface and dipole moment (7.24 D) for the OPE **4** with a fluorinated aromatic ring. Red and blue colors of the surface represent higher and lower electron densities respectively, indicating the high electronegativity that fluorines impart, and the electron-withdrawing nature of the nitro group. For a nonfluorinated OPE (not shown), the vector is smaller (3.1 D).

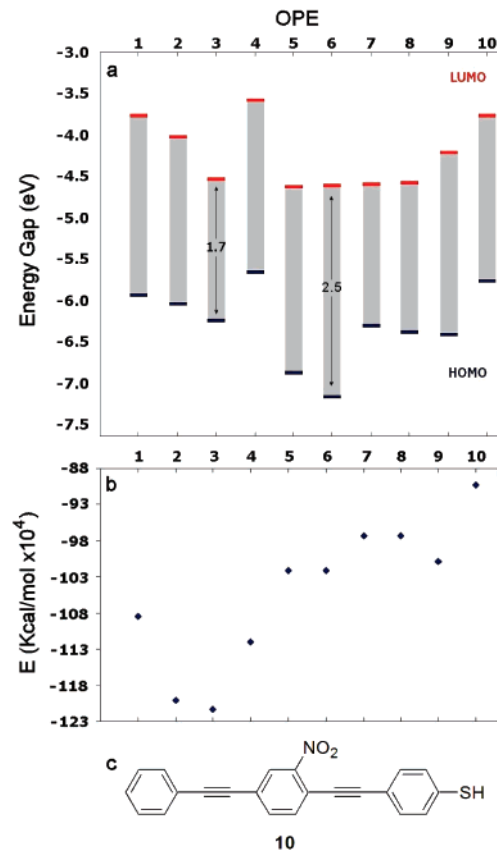
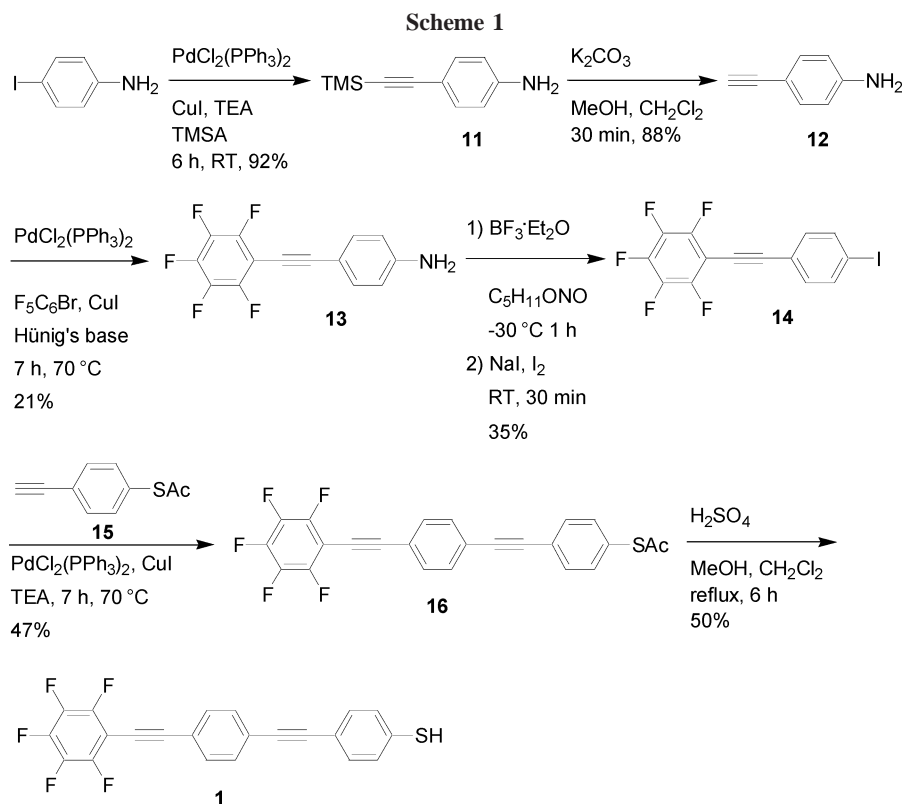


Figure 3. (a) Calculated energy gaps between the frontier orbitals and (b) total energy for every target presented in this work. (c) Chemical structure for OPE **10** included for comparison purposes.

92 nated ring in the opposite direction of the electrode contact
 93 was responsible for reducing the energy barrier, allowing
 94 for a more facile electronic flow.²¹ Using calculations, such
 95 dipole moments were also observed in our new targets as
 96 shown in Figure 2.

97 Figure 3 illustrates calculated energies of targets **1–9** and
 98 the energy gaps of their molecular orbitals. For comparison
 99 purposes, the same calculations were done for 4-(2-nitro-4-
 100 phenylethynylphenylethynyl)benzenethiol **10** (Figure 3c).
 101 Although the OPE **6** shows the largest energy gap, in general
 102 the LUMOs of all the molecules lie at a value equal to or
 103 lower than that of their nonfluorinated counterparts. Fluori-
 104 nated compounds such as **4** may lower the HOMO energy
 105 and the corresponding Schottky energy barrier, increasing
 106 the electron transmission from a bulk contact through the
 107 frontier orbitals of a chemisorbed organic film.²²

- (14) Dirk, S. M.; Tour, J. M. *Tetrahedron* **2003**, *59*, 287.
 (15) Chanteau, S. H.; Tour, J. M. *Tetrahedron Lett.* **2001**, *42*, 3057.
 (16) Li, C.; Zhang, D.; Liu, X.; Han, S.; Tang, T.; Zhou, C.; Fan, W.;
 Koehne, J.; Han, J.; Meyyappan, M.; Rawlett, A. M.; Price, D. W.;
 Tour, J. M. *Appl. Phys. Lett.* **2003**, *82*, 645.
 (17) Seminario, J. M.; De La Cruz, C. E.; Derosa, P. A. *J. Am. Chem. Soc.*
2001, *123*, 5616.
 (18) Campbell, I. H.; Kress, J. D.; Marting, R. L.; Smith, D. L.; Barashkov,
 N. N.; Ferraris, J. P. *Appl. Phys. Lett.* **1997**, *71*, 3528.
 (19) Vondrak, T.; Cramer, C. J.; Zhu, X.-Y. *J. Phys. Chem. B.* **1999**, *103*,
 8915.
 (20) Facchetti, A.; Yoon, M.-H.; Stern, C. L.; Katz, H. E.; Marks, T. J.
Angew. Chem., Int. Ed. **2003**, *42*, 3900.
 (21) Campbell, I. H.; Hagler, A. J.; Smith, D. L.; Ferraris, J. P. *Phys. Rev.*
Lett. **1996**, *76*, 1900.



108 The fluorinated mononitro OPE **2** shows a remarkable
109 lower energy value (-120×10^4 kcal/mol) compared with
110 its counterpart nonfluorinated OPE **10** (-90×10^4 kcal/mol,
111 Figure 3b).

112 **2.2. Synthesis.** The synthesis of OPE **1** is presented in
113 Scheme 1. Commercially available 4-iodoaniline was first
114 coupled with trimethylsilylacetylene (TMSA) to afford **11**,
115 which was then desilylated in alkaline methanol to furnish
116 4-ethynylaniline **12** as previously reported.²³

117 Coupling **12** with bromopentafluorobenzene via Sono-
118 gashira reaction²⁴ furnished aniline **13** which was converted
119 to the iodide **14** in two steps: first, diazotization with isoamyl
120 nitrite and boron trifluoride etherate, followed by iodination
121 with sodium iodide and iodine. A second coupling with the
122 free alkyne of the alligator clip **15**²⁵ gave the thioacetate **16**,
123 followed by its acidic-deprotection with sulfuric acid, yield-
124 ing the desired product **1** as a free thiol.

125 Although most of the synthetic steps gave only moderate
126 yields, their relative simplicity and ease prompted us to use
127 them for the synthesis of several different functionalized
128 central cores and alligator clips. Scheme 2 illustrates the
129 synthesis of the OPE **2** that includes a redox center; the nitro
130 group having its origin as commercially available 2-nitro-
131 aniline. Iodination of this starting material with triethylben-
132 zylammonium iodide dichloride provided **17**.²⁶

133 Aside from the direct iodination of the starting material,
134 we used the same reagents and conditions from the previous
135 OPE synthesis to afford the free alkyne nitroaniline **19**.
136 Palladium-catalyzed coupling with $\text{F}_5\text{C}_6\text{Br}$ afforded the
137 fluorinated aniline **20**, which was then converted to the iodide
138 **21** via diazotization, followed by iodination under typical
139 conditions. A second coupling with 4-ethynylphenylthioace-
140 tate (**15**) gave the mononitro fluorinated oligomer **22**, which
141 was finally deprotected under acidic conditions to yield the
142 free thiol **2**.

143 Intermediate **21** made possible the synthesis of a variety
144 of fluorinated oligomers with different functional groups and
145 alligator clips. Scheme 3 shows the synthesis of an OPE that
146 bears an amino group, an electron-donating moiety that will
147 provide complementary electronic behavior compared to the
148 OPE **2**.²⁵

149 The reduction of the nitro moiety on **21** was accomplished
150 by treatment with tin(II) chloride, affording the iodoaniline
151 **23**. Subsequent coupling with the free alkyne **15** and
152 deprotection of the resulting thioacetate provided the desired
153 aniline **3** as a free thiol.

154 An isomer of the fluorinated-mononitro OPE **2** was
155 prepared as shown in Scheme 4. This time, the pentafluoro
156 aromatic ring was prepared bearing a free alkyne by coupling
157 first with TMSA to give **25**, followed by alkaline deprotec-
158 tion with KOH to obtain **26** as a light clear liquid.²⁷ The
159 iodide intermediate **27**, which was produced by iodinating
160 3-nitroaniline with iodine monochloride, was ready for a
161 Sonogashira coupling with **26**. This different approach
162 unfortunately did not show an increased yield for the

(22) Fan, F. F.; Lai, R. Y.; Cornil, J.; Karzazi, Y.; Brédas, J.-L.; Cai, L.; Cheng, L.; Yao, Y.; Price, D. W., Jr.; Dirk, S. M.; Tour, J. M.; Bard A. J. *J. Am. Chem. Soc.* **2004**, *126*, 2568.

(23) Dirk, S. M.; Price, D. W.; Chanteau, S. H.; Kosynkin, D. V.; Tour, J. M. *Tetrahedron* **2001**, *57*, 5109.

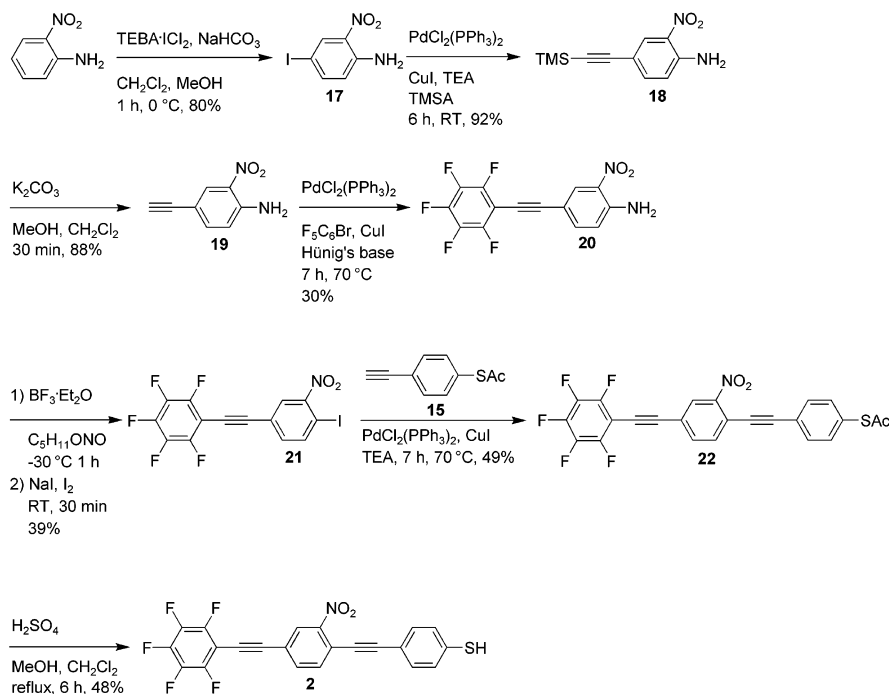
(24) Sonogashira, K.; Tohda, Y.; Hagihara, N. *Tetrahedron Lett.* **1975**, *50*, 4467.

(25) Tour, J. M.; Rawlett, A. M.; Kozaki, M.; Yao, Y.; Jagessar, R. C.; Dirk, S. M.; Price, D. W.; Reed, M. A.; Zhou, C.; Chen, J.; Wang, W.; Campbell, I. H. *Chem. Eur. J.* **2001**, *7*, 5118.

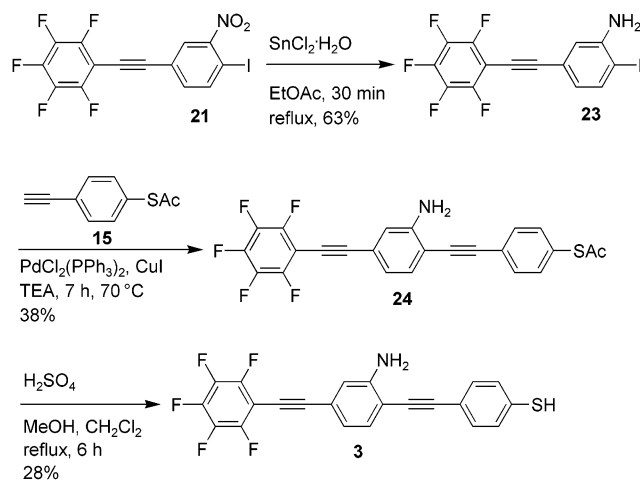
(26) Kosynkin, D. V.; Tour, J. M. *Org. Lett.* **2001**, *3*, 991.

(27) Under the typical deprotection condition of the TMS-acetylene (i.e., dissolved in $\text{CH}_2\text{Cl}_2/\text{MeOH}$ and treatment with K_2CO_3), 4-methoxy-2,3,5,6-tetrafluorophenylethyne was isolated as a white solid.

Scheme 2



Scheme 3



extended aniline **28**, compared to the approach used to prepare the regioisomeric intermediate **20** (Scheme 2). Subsequent iodination was performed under the same diazotization and iodination conditions as previously used, to isolate **29**. Final coupling with the alligator clip **15** and deprotection of the resulting thioacetate yielded the mono-nitro OPE **4** as the free thiol.

Having the regioisomeric intermediates **21** and **29** in hand, it was convenient to couple them with other alligator clips to afford OPEs capable of forming molecule-metal junctions.

Scheme 5 depicts the synthesis of two OPEs with nitrile alligator clips and two OPEs with pyridyl alligator clips, by coupling the iodides **21** and **29** with the corresponding 4-ethynylbenzonitrile **31**¹⁴ and 4-ethynylpyridine **32**,²⁸ affording the desired final OPEs **5–8**. As illustrated in Scheme 6, a third pyridyl-containing OPE **9** with both amine and

nitro functional groups was synthesized. The presence of electron-rich and electron-deficient groups in the same π ring might favor close cofacial π -stacking.²⁹

To synthesize **9**, free alkyne **26** was coupled with the dibromide **33**,²⁵ yielding **34**. Further TMSA-coupling to the remaining bromide afforded **35** and subsequent deprotection of the corresponding alkyne afforded **36**. A final coupling with 4-iodopyridine **37**¹⁵ resulted in the desired pyridine-containing OPE **9**.

Having the free alkyne **36** in hand, we attempted to prepare a free thiol target, as depicted in Scheme 7.

Alligator clip **38** was coupled in a Sonogashira reaction, affording **39**. However, when attempting deprotection of the thioacetate under acidic conditions, the material was too unstable to allow its isolation.³⁰

2.3. Thermal Analysis. Several solution-phase preparations of SAMs for molecular electronics have been developed, and related recent techniques have focused on the deposition of organic thin films,³¹ with a desire toward formation of cleaner intact films of oligomers⁵ and polymers with low⁶ and average molecular weight.³² Gas-phase deposition could be particularly interesting since no solvents are present to coadsorb on the substrate, and our initial use of vapor-phase depositions, under ambient pressure conditions, have led to more uniform and well-ordered SAMs.³³ The use of inert and UHV atmospheres (ca. 10^{-10} Torr) 205

(29) Warner, M. *Crystal Structure Determination*; Teubner: Stuttgart, 1996.

(30) CAUTION! Deprotection of compound **39** on a 4-mmol scale resulted in a violent explosion, which caused permanent damage to surrounding laboratory items. See the Experimental Section and Tour, J. M.; Lamba, J. S. *J. Am. Chem. Soc.* **1993**, *115*, 4935.

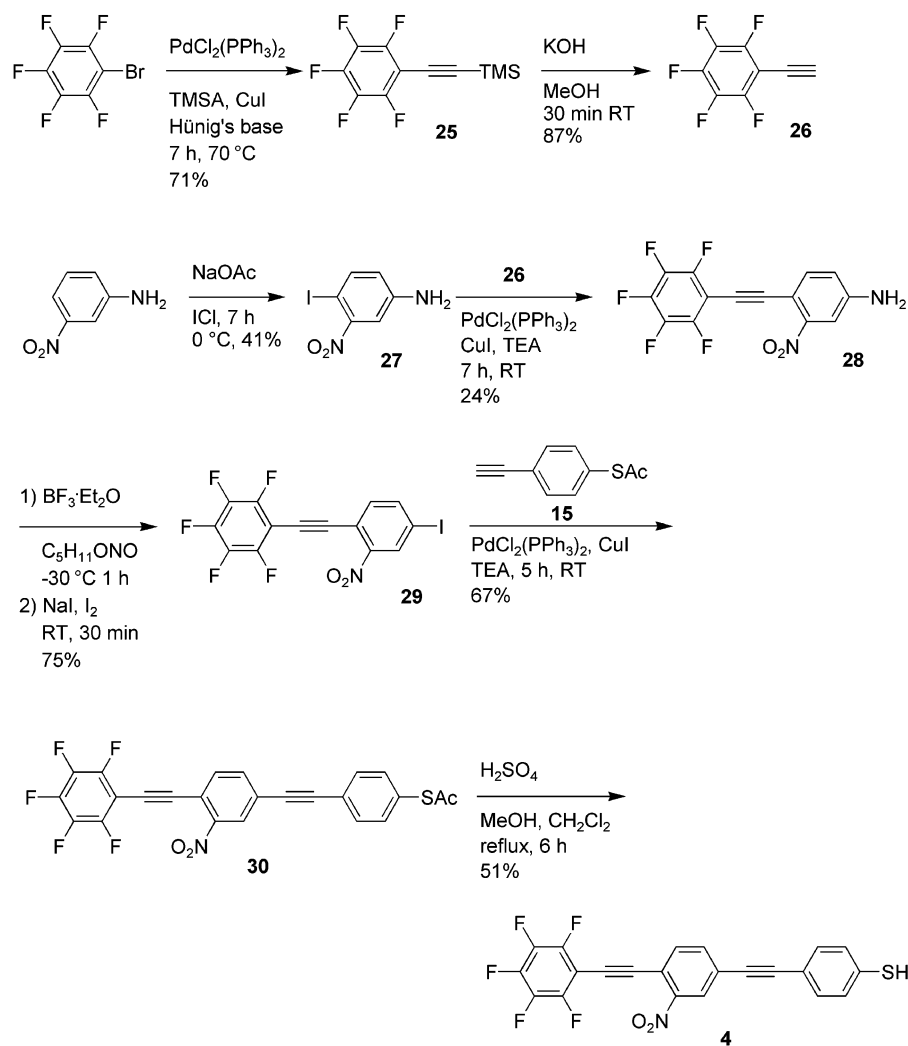
(31) Pique, A.; McGill, R. W.; Chung, R.; Bucaro, M. A. *Thin Film Solids* **1999**, *536*, 355.

(32) Bubb, D. M.; Ringeisen, B. R.; Callahan, J. H.; Galicia, M.; Vertes, A.; Horwitz, J. S.; McGill, R. A.; Houser, E. J.; Wu, P. K.; Pique, A.; Chrisey, D. B. *Appl. Phys. A* **2001**, *73*, 121.

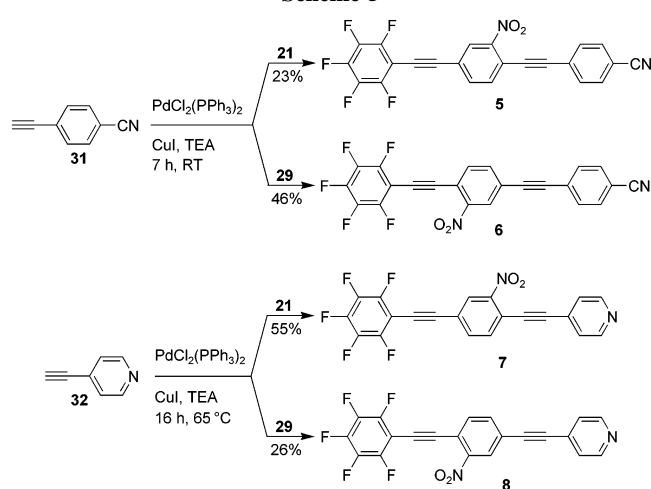
(33) Donhauser, Z. J.; Price D. W., Jr.; Tour, J. M.; Weiss P. S. *J. Am. Chem. Soc.* **2003**, *125*, 11462.

(28) Ziessel, R.; Suffert, J. *Tetrahedron Lett.* **1991**, *32*, 757.

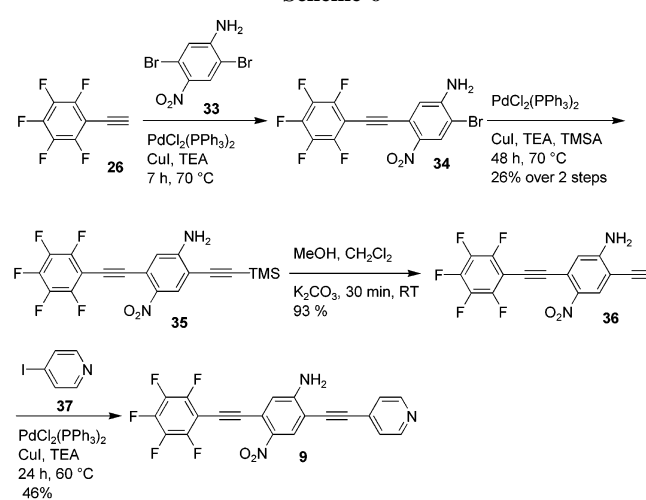
Scheme 4



Scheme 5



Scheme 6



206 should allow molecular components to evaporate at lower
 207 temperatures,³⁴ preserving the original integrity of the
 208 molecular components, while being compatible with state-
 209 of-the-art PVD fabrication processes.

210 With this view in mind, we explored the thermal stability
 211 of our fluorinated OPEs as candidates for vapor phase

(34) A gas chromatography analysis showed that a small amount of compound **1** sublimed at 150 °C under a pressure of 0.05 mmHg.

212 assembly and compared these to the nonfluorinated analogues. DSC can provide an indication of the melting point
 213 noted by a sharp endothermic transition and decomposition
 214 temperature of molecular systems represented by an exothermic
 215 transition. Often a sharp exotherm is related to an
 216 intramolecular event, whereas a broad exotherm is indicative
 217 of cross-linking.³⁵ Figures 4 and 5 show the DSC thermo-
 218 grams for compounds **6** and **7**, respectively, wherein there
 219

Scheme 7

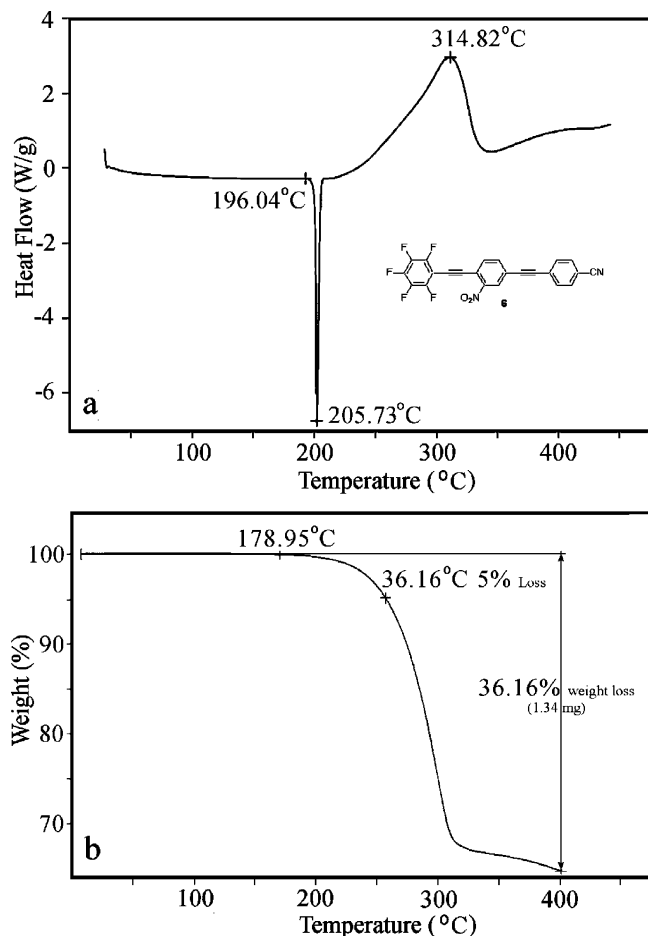
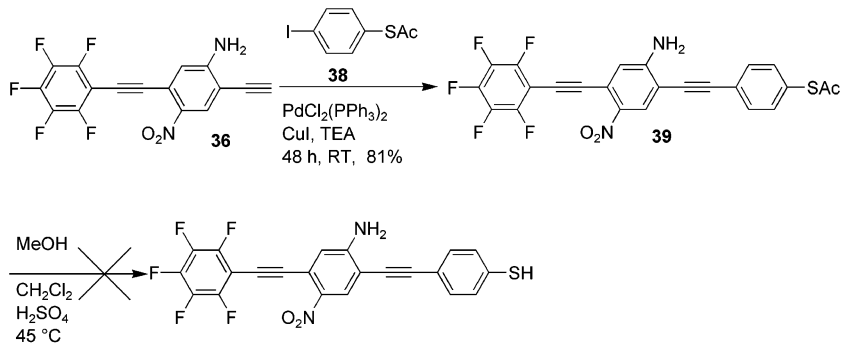


Figure 4. (a) DSC profile for OPE 6, showing an endotherm (melting point) with its lowest point at 205 °C, followed by an exotherm (decomposition) reaching a maximum of 315 °C. (b) TGA profile of the same compound, showing ca. 36% weight loss over a range of 400 °C.

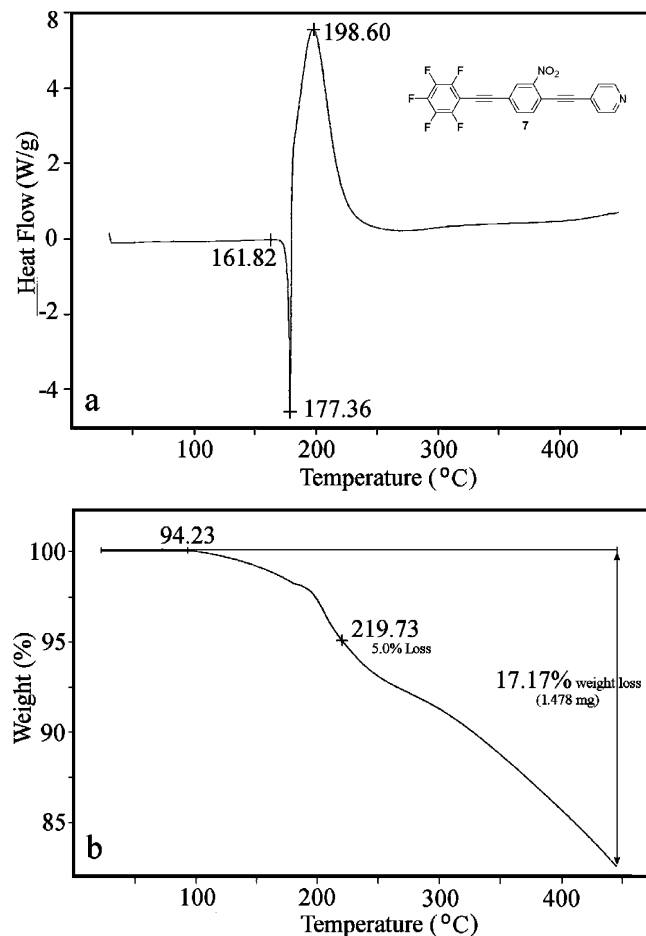


Figure 5. (a) DSC profile for OPE 7, showing an endotherm (melting point) peaking at 177 °C, followed by an exotherm reaching a maximum of 199 °C. (b) TGA profile of the same compound, showing a 17% weight loss over a range of 450 °C.

220 are sharp endothermic events (melting)
 221 222 respectively, followed by broad decomposition (cross-
 223 linking) events.

224 DSC could provide a pre-screen for use of these com-
 225 pounds in vapor deposition device assemblies. Thermogravi-
 226 metric analysis (TGA), which is usually performed at
 227 standard pressure, shows the temperature at which molecu-
 228 lar components evolve from a sample. As expected, the results
 229 (Table 1) showed a common pattern in that the decomposi-
 230 tion temperatures were 30–50 °C higher in the fluorinated
 231 versions.³⁶ Note that the thiols were not tested because of

231 their oxidative instability and risk of reaction with the thermal
 232 analysis pans. Therefore, the fluorinated versions described
 233 here are more thermally stable than their nonfluorinated
 234 analogues, and they would be more amenable to PVD
 235 formation of organic assemblies in UHV.

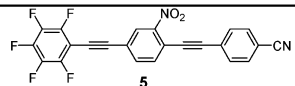
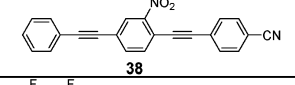
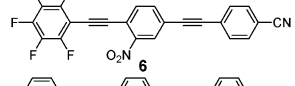
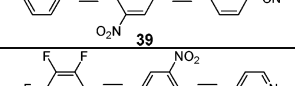
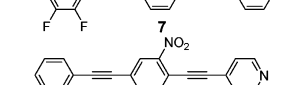
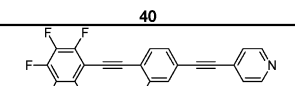
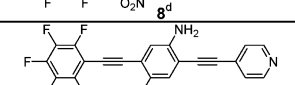
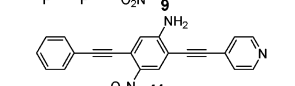
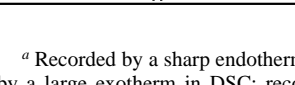
236 **2.4. Monolayer Formation Analysis.** The chemical
 237 integrity at the chemical interface level of the SAMs was
 238 initially verified by single-wavelength ellipsometry (SWE),
 239 contact angle, and cyclic voltammetry (CV).

(35) Stevens, M. P. *Polymer Chemistry, An Introduction*; Oxford University Press: New York, 1999.

(36) Schultz, J.; Bhatt, J.; Chartoff, R. P.; Pogue, R. T.; Ullett, J. S. *J. Polym. Sci. B* **1998**, *37*, 1183.

(37) Chanteau, S. H. *Synthesis of Conjugated Molecules: From Electronics to MolecularART*, Ph.D. Thesis 2003, 41.

Table 1. Thermal Comparison of Fluorinated OPEs vs Non-fluorinated OPEs (Compounds 38,¹⁴ 39,¹⁴ 40,¹⁵ and 41³⁷ were Included for Comparison)

| Compound | Melting Point ^a (°C) | Decomposition ^b (°C) |
|-------------------------------------------------------------------------------------|---------------------------------|---------------------------------|
|  | NO ^c | 160 |
|  | NO ^c | 125 |
|  | 206 | 210 |
|  | 136 | 140 |
|  | 177 | 180 |
|  | 136 | 140 |
|  | 176 | 180 |
|  | NO ^c | 220 |
|  | 101 | 188 |

^a Recorded by a sharp endotherm in DSC; recorded at peak. ^b Recorded by a large exotherm in DSC; recorded at onset. ^c No melting point was observed by DSC. ^d Nonfluorinated version was not synthesized for comparison.

Multiple ellipsometric measurements at different spots on several different samples for each type of SAM were collected, and the resulted average experimental thickness is compared with the theoretical thickness in Table 2. The comparison also includes static (Θ_{stat}) water contact angles for every SAM and hexadecane (HD) contact angles for SAMs from 2 and 3. The water contact angles for the SAMs made from the pyridines 7–9 are slightly higher than the values for a SAM prepared with an analogous nonfluorinated compound 10.^{38,39} The change in hydrophobicity may indicate a SAM with fewer defects.⁴⁰ The very low HD contact angles indicate that SAMs 2 and 3 are disordered.^{40a} Except for the nitriles 5 and 6,⁴¹ the rest of the compounds achieved a close (but not full) SAM formation within 24 h.

(38) Stapleton, J. J.; Harder, P.; Daniel, T. A.; Reinard, M. D.; Yao, Y.; Price, D. W.; Tour, J. M.; Allara, D. L. *Langmuir* **2003**, *19*, 8245.

(39) Furthermore, we found that the contact angle of a SAM made of 4 can be increased from 85.1° to 93.6° by changing EtOH/CH₃CN to CH₂Cl₂ as a solvent during the SAM preparation.

(40) (a) Bain, C. D.; Troughton, E. B.; Tao, Y.-T.; Evall, J.; Whitesides, G. M.; Nuzzo, R. G. *J. Am. Chem. Soc.* **1989**, *111*, 321. (b) Bain, C. D.; Evall, J.; Whitesides, G. M. *J. Am. Chem. Soc.* **1989**, *111*, 7155. (c) Zehner, R. W.; Sita, L. R. *Langmuir* **1997**, *13*, 2973.

(41) A dominance of a η^2 - (i.e., π - or side-on) over a η^1 -coordination (or σ -bonding via the N) through the triple bond and the surface, could be responsible for lower SAM thicknesses using compounds 5 and 6; see Steiner, U. B.; Caseri, W. R.; Suter, U. W. *Langmuir* **1992**, *8*, 2771.

Table 2. Comparison of Theoretical and Experimental Thicknesses, and Static Contact Angle Goniometry (Θ_{stat}) of SAMs Made of Compounds 1–9

| entry | compound | SWE ^a (Å) | | Θ_{stat} ^d | |
|-------|----------------------|--------------------------|--------------|------------------------------|----|
| | | theoretical ^b | experimental | H ₂ O | HD |
| 1 | 1–SAM ^e | 21 | 16 | 90.7 | |
| 2 | 2–SAM ^e | 21 | 17 | 87.7 | 10 |
| 3 | 3–SAM ^e | 21 | 14 | 89.2 | 0 |
| 4 | 4–SAM ^g | 20 | 15 | 93.6 | |
| 5 | 5–SAM ^{f,g} | 20 ^c | 13 | 85.6 | |
| 6 | 6–SAM ^g | 20 ^c | 13 | 83.9 | |
| 7 | 7–SAM ^g | 18 | 16 | 88.9 | |
| 8 | 8–SAM ^g | 18 | 15 | 85.8 | |
| 9 | 9–SAM ^g | 18 | 14 | 90.3 | |

^a Within $\pm 10\%$ of error. ^b At 20° to surface normal angle. ^c Pt–N bond length taken as 1.13 Å. ^d $\pm 3^\circ$. ^e SAMs on Au. ^f Using CH₂Cl₂ as solvent for SAM formation, see ref 39. ^g SAMs on Pt.

Compared with our recent work with analogous nonfluorinated compounds such as 10,³⁸ the experimental thicknesses values reported in Table 2 may indicate lower order in the SAM formation, despite literature that indicates otherwise.¹⁹ However, the tilt angle may be $>20^\circ$ from the surface normal, therefore bringing the experimental data more in concert with the calculated thicknesses. Also, longer reaction times and more suitable solvents may allow for the formation of full and closer-packing SAMs. The measured film thicknesses averaged about 70% of the theoretical values.

Additional characterization of the average compactness and extent of structural defects of SAMs on electrodes was determined by CV following a previously reported technique.⁴² Comparison of redox currents of an electroactive species, for example ferricyanide [Fe^{III}(CN)₆³⁻] used in this study, on bare electrodes and on electrodes coated with SAMs, gives a good indication of the surface coverages of the SAMs. Due to the passivation effect from the molecular monolayer, decreased redox currents are expected on the SAMs-coated electrodes. Figure 6 shows CVs of bare electrodes and electrodes self-assembled with compounds 1, 4, and 5, in solutions of 1 mM K₃[Fe(CN)₆] and 0.1 M KCl. The CVs show a good current passivation by SAMs of the adsorbates 1 on Au and 4 on Pt electrodes, whereas the assembly of compound 5 on Au electrode indicated partial passivation. In all cases the SAMs at least partially inhibited transport of the active ion ferricyanide to the metal surface under the CV conditions.⁴³ The CV results support our previous observations for similar oligomers.^{38,44}

2.5. Chemical Interface Analysis. A closer examination of the chemical composition of the SAM was pursued with a series of XPS experiments. Figure 7 summarizes high-resolution XPS multiplets for the C1s region of SAMs on Au prepared with compounds 1–4.

The signal is clearly made of two different peaks. The main component, the nonfluorinated carbons from the aromatic ring, lies at the binding energy of ca. 284.5 eV (Figure 7, light blue peak), while the higher energy of the

(42) Cheng, L.; Yang, J.; Yao, Y.; Price, D. W., Jr.; Dirk, S. M.; Tour, J. M. *Langmuir* **2004**, *20*, 1335.

(43) Fan, F.-R.; Yao, Y.; Cai, L.; Cheng, L.; Tour, J. M.; Bard, A. J. *J. Am. Chem. Soc.* **2004**, *124*, 4035.

(44) Maya, F.; Flatt, A. K.; Stewart, M. P.; Shen, D. E.; Tour, J. M. *Chem. Mater.* **2004**, *16*, 2987.

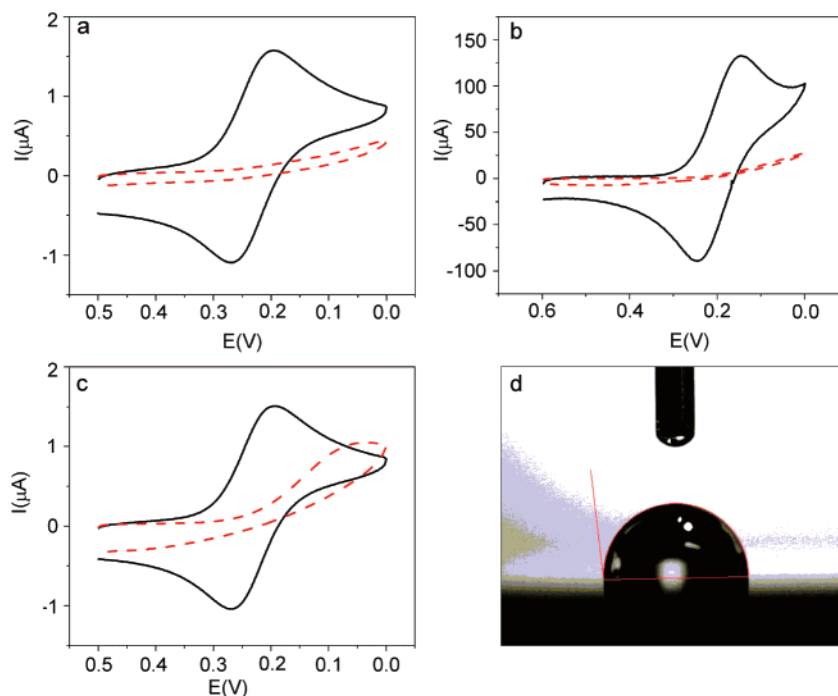


Figure 6. Cyclic voltammograms in a solution of 1 mM $K_3[Fe(CN)_6]$ and 0.1 M KCl on bare electrodes (solid lines) and SAM-coated electrodes (curved lines): (a) compound **1** on Au, (b) compound **4** on Pt, and (c) compound **5** on Au. Potentials were reported vs a silver/silver chloride reference electrode (Ag|AgCl) in plots (a) and (c), but a saturated calomel reference electrode (SCE) in plot (b). Scan rate was 0.1 V/s at an initial negative scan direction. The Au disk electrodes used for plots (a) and (c) have a diameter of 1 mm, whereas the Pt electrode has a diameter of 9 mm. (d) Contact angle profile of a 20- μ L drop of water on SAM of **4** on Pt.

293 second peak is characteristic of the more electron-deficient
294 fluorinated aromatic ring (Figure 7, dark blue peak).

295 The split of the carbon signal into two well-defined peaks,
296 their relative ratios, and their binding energies, were con-
297 sistent in all the cases and with our previous XPS analyses
298 of similar fluorinated oligomers.^{44,45} Deconvolution of the
299 carbon signal allowed the elucidation of a third component
300 at ca. 285.7 eV for every SAM (Figure 7, pink peak). For
301 the carbon region, the ratio of this third peak relative to the
302 other two peaks varies on every SAM, having a direct
303 relationship to the number of carbons adjacent to electron-
304 deficient carbons bearing electronegative atoms (as F, and
305 N for the $-NO_2$ and $-NH_2$ functional groups).

306 The third type of carbon includes the C–S carbon (Figure
307 7, pink peak) from the alligator clip. Using this correlation,
308 the theoretical ratio for the three carbon peaks of SAM-**1** is
309 (fluorinated carbon/adjacent carbons/nonfluorinated carbons)
310 5:2:15, while the deconvolution in Figure 7 for the three
311 carbon peaks on the same SAM gives an experimental ratio
312 of 5:1.8:15. The similarity of the theoretical to the experi-
313 mental ratios of the three carbon types for all SAMs is
314 evidence for the integrity of the molecular thin film on the
315 surface. Furthermore, XPS survey spectra (not shown) for
316 all the SAMs showed the absence of chemical elements that
317 were not part of the oligomers. Although these analyses are
318 for SAMs formed in solution, we can capitalize on the high
319 thermal stability of the fluorinated oligomers for their use
320 in PVD processes, expecting to observe a good chemisorption
321 of the oligomers as we have seen with vapor phase annealing

of alkanethiolate SAMs.³³ High-resolution XPS multiplex for
the N and S region were also acquired for SAMs made of
compounds **1–4** as shown in Figure 8, while the signals for
the N region on SAMs made of the pyridines **7–9** are
collected in Figure 9. Table 3 summarizes the binding
energies, the relative concentrations of the SAMs, and the
chemical species of interest.

From Figure 8, it is worth noting the second signal on
SAM-**2** for the N1s region, assigned to an aromatic amine
group, from a SAM made with the compound **22** (the
thioacetyl-protected precursor of compound **2**) that has no
other functional group on its central ring but a nitro. The
presence of the amine originates from the reduction of the
nitro group when the oligomer **22** was assembled under basic
conditions, as shown previously.³⁸ The S2p signal (Figure
8, right side) contained a doublet centered at ca. 163 eV
corresponding to the S covalently attached to the Au surface.
When compared with previous work,⁴⁴ S chemisorbed on
Au was the main component in the S region for all SAMs,
observing little or no signal for unreacted thioacetate or thiol.
Figure 9 shows the N region from SAMs formed with
pyridines **7–9**, with a main signal at ca. 400 eV, corre-
sponding to the pyridyl N. In case of compound **9** as
chemisorbate, the signals from the pyridyl and the amino
groups coincide. For all the SAMs, a small component with
a higher binding energy of 405.6 eV is assigned to the nitro
group (Figure 9 and Table 3). On the basis of results shown
in Figures 8 and 9, we observed that free thiols (and not the
thioacetyl-protected versions) such as **2** allowed for direct
assembly on Au, with no need for the deprotection step, and
more importantly, the integrity of the adsorbed organic film
was maintained.⁴⁷

(45) Stewart, M. P.; Maya, F.; Kosynkin, D. V.; Dirk, S. M.; Stapleton, J. J.; McGuinness, C. L.; Allara, D. L.; Tour, J. M. *J. Am. Chem. Soc.*, **2004**, *126*, 370.

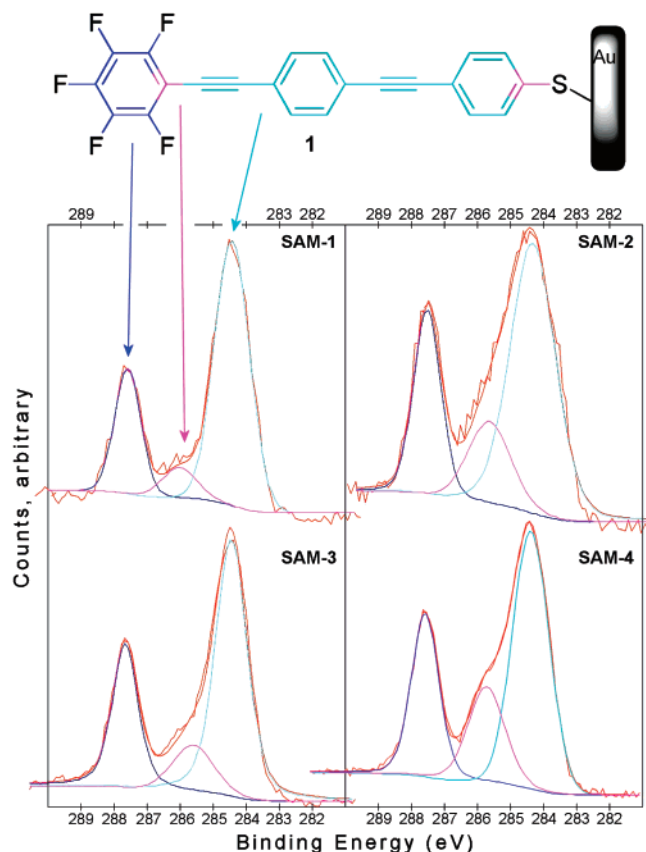


Figure 7. High-resolution XPS multiplex for the C1s region of SAMs on Au of compounds 1–4. In all four SAMs, two main components at ca. 284.5 eV (right peak in light blue) and 287.7 eV (left peak, dark blue) correspond to the nonfluorinated and fluorinated Cs respectively; while a third component (pink) is evident only after deconvolution. The chemical structure of chemisorbed **1** shows the assignment of the three peaks to the different carbons (nonfluorinated carbons, light blue; fluorinated carbons, dark blue; and adjacent carbons, pink) from the molecular backbone. XPS pass energy was 11.75 eV in a 45° takeoff angle. The Au 4f_{7/2} binding energy of 84.00 eV was taken as a reference for all SAMs.

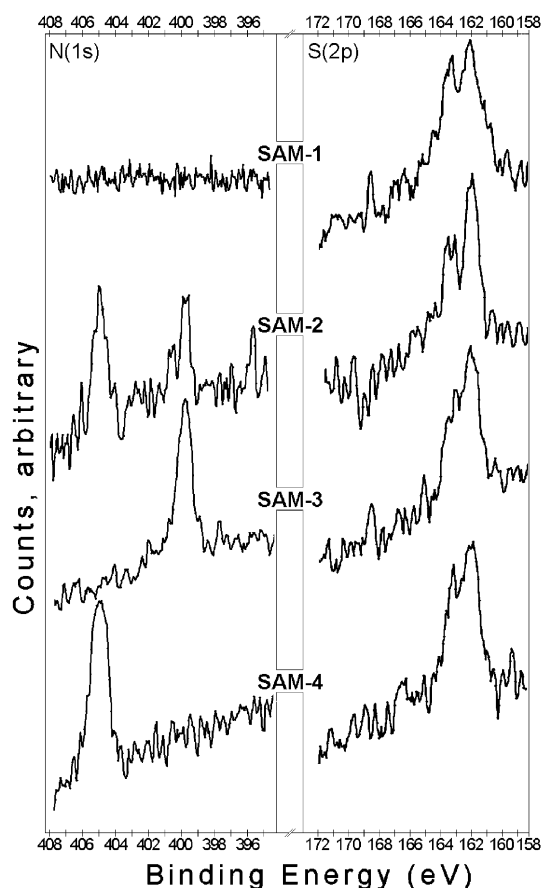


Figure 8. High-resolution XPS multiplex for the N1s and S2p regions (left and right columns, respectively) of SAMs on Au of compounds 1–4 after a 24 h assembly time; the N region of SAM-1 was included for comparison. For the SAM-2, note the presence of two peaks assigned to nitro and amine groups in a ca. 1:1 ratio. XPS pass energy was 11.75 eV at a 60° takeoff angle. The Au 4f_{7/2} binding energy of 84.00 eV was taken as a reference for all SAMs.

To complement our analyses at the chemical interface, FTIR analysis was done to gain more data on the physical characteristics of the adsorbed organic films. Figure 10 shows the spectrum of a grazing-angle FTIR experiment (inset a), with the structural features related to the chemisorbed **4** on Pt, providing information about its intact presence on the surface. Comparable features are present in both the IR absorption of SAM-4 (Figure 10a) and the KBr pellet spectrum of the compound **4** (Figure 10b).

A weak aromatic stretching band $\nu_{\text{as}}(\text{C}-\text{H})$ is present at 3083 cm⁻¹ for the KBr pellet spectrum (Figure 10b), as well as a moderately weak S–H mode $\nu_{\text{as}}(\text{SH})$ at 2562 cm⁻¹. A weak band at 2209 cm⁻¹ in the KBr pellet spectrum (Figure 10b) represents the absorption of the triple bond, which is also seen with a very weak intensity in the grazing-angle spectrum (Figure 10a). Plane ring breathing $\nu(\text{C}=\text{C})$ modes at 1548 and 1499 cm⁻¹ can be seen in the SAM on Pt (Figure 10a), absorbing near the antisymmetric NO₂ stretch $\nu_{\text{as}}(\text{NO}_2)$

mode at 1526 cm⁻¹ and the symmetric NO₂ stretch $\nu_{\text{s}}(\text{NO}_2)$ mode at 1445 cm⁻¹. At lower wavenumbers, an in-plane aromatic C–H deformation $\nu_{\text{ip}}(\text{C}-\text{H})$ mode at 996 cm⁻¹ is present in both spectra of Figure 10, as well as an out-of-plane aromatic C–H deformation $\nu_{\text{op}}(\text{C}-\text{H})$ mode at 923 cm⁻¹ with a weak intensity.

Combined with the surface analysis data, this comparison of FTIR spectra provides clear evidence for the integrity of organic films made from electron-deficient fluorinated OPEs.

3. Summary

We present the synthesis of new OPEs that contain a polyfluorophenyl ring and various alligator clips, including pyridines, nitriles, or free thiols, with no need for further deprotection to achieve chemisorption. Calculations at the DFT level indicate that the pentafluoro aromatic ring produces a strong dipolar moment directed away from the alligator clip. The synthetic design of OPEs 1–9 includes redox centers, features that have been found to be important in prior work from this lab.² Thermal analysis by DSC and TGA showed higher thermal stability for the fluorinated OPEs. Goniometry, IR, and X-ray photoelectron spectroscopy confirm the ability of these new fluorinated oligomers, synthesized as free thiols, to form SAMs on Au and Pt

(46) Ng, S. S.; Chan, H. S. O.; Lu, G.-F. *Macromolecules* **2003**, *36*, 1543.

(47) The comparison of the XPS signals at the N1s region from a SAM made of **22** and a SAM made of **2**, as well as signals from SAMs made of pyridines **7–9**, allowed us to confirm that the reduction of the nitro group was not the result of a chemical degradation caused by the emission of the electrons upon X-ray excitation during the XPS analysis.

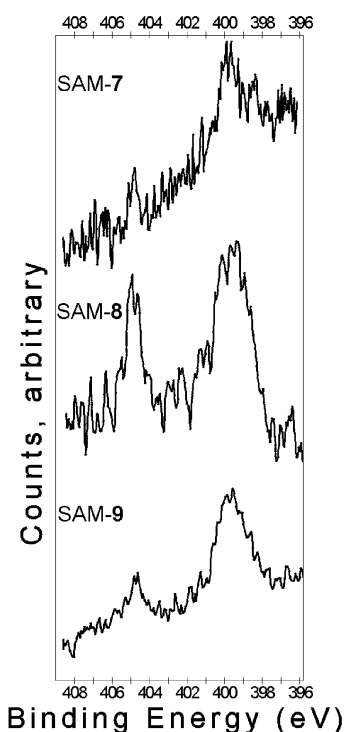


Figure 9. High-resolution XPS multiplex for the N1s region of SAMs made with compounds 7–9 on Pt for 24 h. XPS pass energy was 11.75 eV in a 60° takeoff angle. The Pt 4f_{7/2} binding energy of 71.00 eV was taken as a reference for all SAMs.

surfaces. From these experimental and theoretical results, it is logical that fluorinated OPEs would be good candidates for SAM formation processes using PVD. The electrical and thermal testing of these targets for further fabrication of molecular-based architectures is a work in progress.

4. Experimental Section

4.1. Thermal Analyses. TGA was performed in a TA Q₅₀ TGA7 30–400 °C or 30–800 °C at 10 °C/min under N₂ gas. For experiments heating to 400 °C, aluminum pans were used, whereas for experiments at higher temperatures, platinum pans were used. DSC was performed with a TA Q₁₀ using a 30–450 °C scanning window at 10 °C/min under N₂ gas.

4.2. Gold Substrates. Gold films were deposited by thermal evaporation of a 200-nm-thick Au layer onto Si wafers with a 25-nm Cr adhesion layer at a rate of 1 Å/s at 2 × 10⁻⁶ Torr. Before use, the Au substrates were cleaned by a UV/O₃ cleaner (Boeckel Industries, Inc., model 135500) for 10 min to remove organic contamination, and submerged in ethanol for 10 min before being dried in flowing N₂. This procedure was used to provide a reproducibly clean Au surface.^{48,49} The Pt substrates for FTIR measurements were prepared and provided by Z. Li of Hewlett-Packard laboratories, Palo Alto, CA.

4.3. Self-Assembly. The oligomer as free thiol (1 mg) was dissolved in the corresponding solvent (3–4 mL). When the thioacetyl-protected intermediate was used, concentrated NH₄OH (10 μL) was added prior to a 10-min incubation at room temperature to deprotect the thiol group. Unless otherwise stated, the cleaned substrates (Au or Pt) were immersed into the adsorbate solution at room temperature for a period of 24 h, followed by 5 h at 40 °C to promote closer molecular packing, the same methodology used in

our previous work.^{33,34} All the solutions were freshly prepared, previously purged with N₂ for an oxygen-free environment, and kept in the dark during immersion to avoid photooxidation. After assembly, the samples were removed from the solution, rinsed thoroughly with EtOH then acetone, and blown dry with N₂.

4.4. SWE Measurements. Measurements of surface optical constants and molecular layer thicknesses were taken with a single-wavelength (632.8 nm laser) Gaertner Stokes ellipsometer. The n_s and k_s values were the result of several measurements recorded for every clean substrate and used for their corresponding SAM-adsorbed sample. The refractive index was $n_f = 1.55$ for all compounds ($k_f = 0$).⁵⁰

4.5. Contact Angle Goniometry. Static contact angle was measured using a Rame-Hart 2001 apparatus. A 20-μL drop of ultrapure water was dispensed onto the surface using a flat-tipped micrometer syringe. Images of the drop were captured digitally using a CCD camera, and contact angles were analyzed using the RHI 2001 software.

4.6. CV-Monitored Electrode Passivation. The electrochemistry experiments were carried out using a BAS CV-50W voltammetric analyzer (Bioanalytical Systems, Inc). A conventional three-electrode cell was used with a Au or Pt substrate as the working electrode with surface area of 1 cm², with a Pt wire as the counter electrode, and a Ag/AgNO₃ (10 mM AgNO₃ and 0.1 M Bu₄NBF₄ in acetonitrile) as the reference electrode. The scan rate was 0.1 V/s at 23 °C with an initial scan direction that was negative. Self-assembly on the working electrode was performed in an organic solution of 1 mM of the corresponding oligomer.

4.7. XPS Measurements. A Physical Electronics (PHI 5700) XPS/ESCA system at 3 × 10⁻⁹ Torr was used for photoelectron spectra acquisition. A monochromatic Al X-ray source at 350 W was used with an analytical spot size of 800 μm. Takeoff angles of 60 and 45° were used, with a pass energy of 11.75 eV. The Au 4f_{7/2} binding energy of 84.00 eV and the Pt 4f_{7/2} binding energy of 71.00 eV were taken as references.

4.8. Calculations. Total energies, dipole moments, and HOMO/LUMO energies were calculated using Spartan 5.1.⁵¹ The oligomers' structures were geometry minimized at the modified neglect of diatomic overlap (MNDO) level previous to an optimization at the density functional theory (DFT) level.

4.9. FTIR Measurements. A Nicolet Nexus 860 FTIR bench with an MCT/A detector, and SMART SAGA grazing angle accessory (Thermo Electron) fixed at 80° angle of incidence, were used to measure infrared spectra from an organic layer on Pt. Samples used a plasma-cleaned Pt wafer as background. Sample spectra were averaged over 1000 scans at 2 cm⁻¹ resolution.

4.10. Material and General Procedures. Unless stated otherwise, reactions were performed in dry, nitrogen-flushed glassware, using freshly distilled solvents. Reagent-grade diethyl ether (Et₂O) and tetrahydrofuran (THF) were distilled from sodium benzophenone ketyl. *N,N*-Diisopropylethylamine (Hünig's base) and triethylamine (TEA) were distilled from calcium hydride. Reagent-grade acetone, *n*-hexanes, methylene chloride (CH₂Cl₂), methanol (MeOH), ethanol (EtOH), and ethyl acetate (EtOAc) were used without further distillation. Trimethylsilylacetylene (TMSA) was donated by FAR Research Inc. Bromopentafluorobenzene was purchased from Oakwood Chemical Products, Inc. All other commercially available reagents were purchased from Acros Organics and used as received. Unless otherwise noted, reactions were magnetically

(48) Ron, H.; Matlis, S.; Rubinstein, I. *Langmuir* **1998**, *14*, 1116.

(49) Ron, H.; Rubinstein, I. *J. Am. Chem. Chem. Soc.* **1998**, *120*, 8486

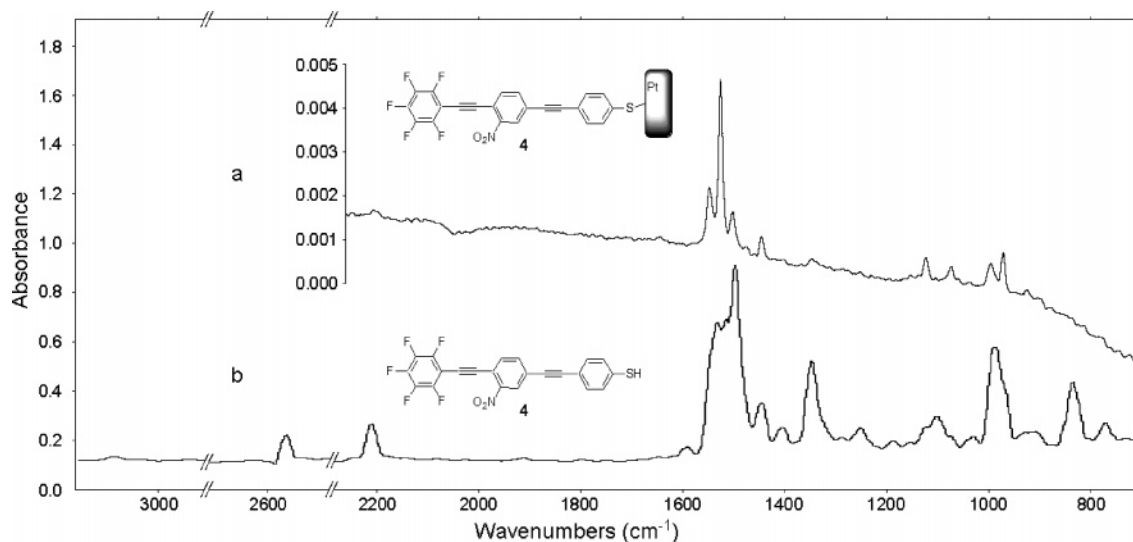
(50) Tour, J. M.; Jones, L.; Pearson, D. L.; Lamba, J. S.; Burgin, T. P.; Whitesides, G. W.; Allara, D. L.; Parikh, A. N.; Atre, S. V. *J. Am. Chem. Soc.* **1995**, *117*, 9529.

(51) *Spartan version 5.1*; Wavefunction, Inc., 18401 Von Karman Avenue, Suite 370, Irvine, CA 92612.

Table 3. Binding Energies and Relative Concentrations for the Chemical Species of Interest, Observed by XPS on SAMs Formed with Compounds 1–9^a

| compound | binding energy (eV) ^b | | | | relative concentration (%) ^c | | | |
|----------------------|----------------------------------|------------------|----------------------------|-----------------------|-----------------------------------------|-------|-------|-------|
| | F(1s) | N(1s) | C(1s) | S(2p ^{1/2}) | F(1s) | N(1s) | C(1s) | S(2p) |
| 1–SAM ^d | 687.98 | | 287.58 286.05 284.41 | 162.05 | 17.35 | | 51.48 | 4.18 |
| 2–SAM ^{d,e} | 688.17 | 405.70 400.00 | 287.85 286.20 284.64 | 162.01 | 21.79 | 4.51 | 49.64 | 2.48 |
| 3–SAM ^d | 687.86 | 399.17 | 287.49 285.70 284.28 | 162.12 | 19.42 | 3.55 | 52.09 | 2.09 |
| 4–SAM ^f | 687.93 | 405.60 | 287.55 285.43 284.37 | 162.23 | 19.61 | 4.33 | 49.71 | 3.21 |
| 5–SAM ^d | 688.26 | 405.65 399.41 | 288.21 285.93 284.43 | | 4.43 | 8.40 | 34.99 | |
| 6–SAM ^d | 687.92 | 405.68 399.46 | 287.52 285.97 284.36 | | 4.09 | 5.36 | 39.48 | |
| 7–SAM ^g | 688.36 | 405.84 398.99 | 287.99 285.43 284.37 | | 8.48 | 5.92 | 38.90 | |
| 8–SAM ^g | 688.31 | 405.82 399.70 | 287.96 285.81 284.48 | | 4.91 | 4.32 | 43.29 | |
| 9–SAM ^g | 688.20 | 405.76 399.41 | 287.77 285.66 284.42 | | 9.06 | 8.17 | 43.84 | |

^a SAM formation was promoted in THF/EtOH or CH₂Cl₂ as solvents for 24 h at room temperature, plus 4 h at 40 °C. When a thioacetyl-protected compound was used, an initial incubation with NH₄OH for 10 min was needed; see ref 43. The Au 4f_{7/2} binding energy of 84.00 eV and the Pt 4f_{7/2} binding energy of 71.00 eV were taken as references. ^b Values with ±0.2 eV of error. ^c Values with ±2% of error; for entries 1–4 Au comprises the remainder of the measured elements, while for entries 5–9 Pt comprises the remainder of the measured elements. ^d THF/EtOH 1:1 used as solvent for SAM formation. ^e Thioacetyl-protected compound **22** used and deprotected in situ with NH₄OH; see ref 43. ^f CH₂Cl₂ used as solvent for SAM formation. ^g THF used as solvent for SAM formation.

**Figure 10.** Comparison of (a) a grazing angle spectrum of a SAM made of compound **4** on platinum, with (b) a KBr pellet absorption of the same compound as a free thiol.

484 stirred and monitored by thin-layer chromatography (TLC) using
485 E. Merck silica gel 60 F₂₅₄ precoated plates (0.25-mm). In general,
486 the chromatography guidelines reported by Still were followed.⁵²
487 Flash chromatography (silica gel) was performed with the indicated
488 solvent systems using silica gel grade 60 (230–400 mesh). ¹H and
489 ¹³C NMR spectra were observed at 400 and 100 MHz, respectively,
490 on a Bruker Avance 400 spectrometer. NMR chemical shifts values
491 for deuterated solvents were followed as reported.⁵³ IR spectra were
492 obtained on a Nicolet Avatar 360 FTIR. Mass spectroscopy was

performed at the Rice University mass spectroscopy lab. All new 493
compounds were named using the Beilstein AutoNom application 494
of Beilstein Commander 2000 software. 495

**4.11. General Procedure for the Coupling of a Terminal 496
Alkyne with an Aryl Halide Utilizing a Palladium–Copper 497
Cross-Coupling (Castro–Stephens/Sonogashira Protocol),²⁴ To 498
an oven-dried screw cap tube or a round-bottom flask equipped 499
with a magnetic stir bar were added the aryl halide, bis(triphenyl- 500**

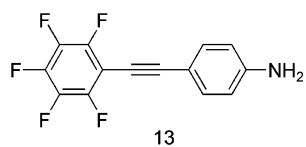
(52) Still, W. C.; Kahn, M.; Mitra, A. *J. Org. Chem.* **1978**, *43*, 2923.(53) Gottlieb, H. E.; Kotlyar, V.; Nudelman, A. *J. Org. Chem.* **1997**, *62*, 7512.

501 phosphine)palladium(II) dichloride (5 mol % based on aryl halide),
502 and copper(I) iodide (10 mol % based on aryl halide). The vessel
503 was sealed with a rubber septum, evacuated, and backfilled with
504 N₂ (3×). THF was added followed by Hünig's base or TEA. The
505 terminal alkyne was then added and the reaction was heated if
506 necessary. The reaction vessel was cooled to room temperature and
507 the mixture was quenched with water or a saturated solution of
508 NH₄Cl. The organic layer was diluted with organic solvent and
509 washed with a saturated solution of NH₄Cl (3×). The combined
510 aqueous layers were extracted with organic solvent (3×), dried over
511 anhydrous MgSO₄, and the solvent was removed in vacuo. The
512 crude product was then purified by flash chromatography.

513 **4.12. General Procedure for Alkaline Deprotection of Tri-**
514 **methylsilyl-Protected Alkynes.** Unless stated otherwise, the TMS-
515 protected alkyne was dissolved in organic solvent and added to an
516 open round-bottom flask equipped with a stirring bar and a solution
517 of potassium carbonate in MeOH, or tetrabutylammonium fluoride
518 (TBAF) buffered with a mixture of acetic acid (AcOH) and acetic
519 anhydride (Ac₂O). THF or CH₂Cl₂ was added to dissolve the organic
520 compound. The reaction was monitored by TLC every 5 min until
521 deprotection was complete. The reaction was quenched with water
522 and extracted with organic solvents (3×). The combined organic
523 layers were dried over anhydrous MgSO₄ and the solvent was
524 removed in vacuo. The crude product was then purified by flash
525 chromatography.

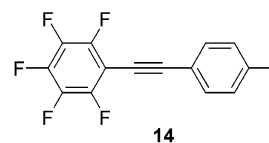
526 **4.13. General Procedure for Iodination of Anilines via**
527 **Diazotization.**²⁶ To an oven-dried round-bottom flask equipped with
528 a magnetic stir bar inside a glovebox was added NOBF₄ (1.1 equiv
529 per aniline). CH₃CN was added to dissolve the salt and cooled to
530 -30 °C. Separately, into an oven-dried round-bottom flask equipped
531 with a magnetic stir bar was added the aniline which had been
532 dissolved in a minimum amount of CH₃CN and/or THF. The
533 organic solution was transferred dropwise via cannula and the
534 temperature was allowed to rise to 0 °C. Et₂O was slowly added
535 until a precipitate crashed out from the slurry. The precipitate was
536 collected by filtration, washed with Et₂O (3×), and dried in vacuo.
537 As an alternative procedure, NOBF₄ was replaced by the use of
538 BF₃·Et₂O (4 equiv per aniline) and isoamyl nitrite (3.5 equiv per
539 aniline) was added to the solution of the aniline in CH₃CN and/or
540 THF. The resulting precipitate was immediately dissolved in CH₃-
541 CN before a slow addition of NaI (2 equiv) and I₂ (1.5 equiv) as
542 a solid mixture. After 30 min, the reaction mixture was dissolved
543 in CH₂Cl₂ and a saturated solution of Na₂S₂O₃ was added until the
544 dark solution turned clearer. The organic layer was washed with
545 water, and after extraction with CH₂Cl₂, the organic layers were
546 collected and dried over MgSO₄, and the solvent removed in vacuo
547 for further purification.

548 **4.14. General Procedure for Acid-Deprotection of Arylthio-**
549 **acetates.** In an oven-dried round-bottom flask equipped with a
550 magnetic stir bar, the arylthioacetate was dissolved in equal amounts
551 of CH₂Cl₂ and degassed MeOH. The solution was acidified with a
552 small volume of H₂SO₄, and the reaction mixture was allowed to
553 reflux for 4 h. After cooling, the crude mixture was dissolved in
554 CH₂Cl₂ and washed with water. Extractions with CH₂Cl₂ were
555 followed by drying over MgSO₄ and removal of the solvents in
556 vacuo for further purification.

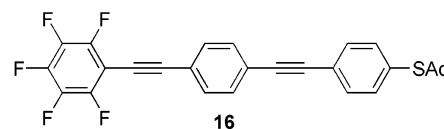


557 **4.15. 4-(4-Pentafluorophenylethynyl)phenylamine (13).** Following
558 the Sonogashira coupling protocol, bromopentafluorobenzene (19.0

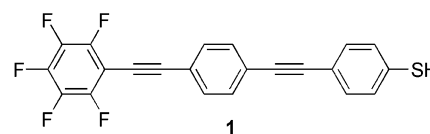
g, 77.0 mmol), 4-ethynylaniline **12**²³ (9.0 g, 77.0 mmol), PdCl₂-
(PPh₃)₂ (2.7 g, 3.8 mmol), and CuI (1.5 g, 7.7 mmol) were dissolved
in THF (150 mL). Hünig's base (54.0 mL, 307.0 mmol) was added
and the reaction was stirred overnight at 70 °C. Purification by
flash chromatography (CH₂Cl₂) afforded the desired product (4.4
g, 21% yield) as a dark yellow solid; mp 133–137 °C. IR (KBr)
3483, 3394, 2605, 2566, 2208, 1610, 1522, 1445, 1291, 1176 cm⁻¹.
¹H NMR (400 MHz, CDCl₃) δ 7.38 (m, 2H), 6.65 (m, 2H), 3.93
(br s, 2H). ¹³C NMR (100 MHz, CDCl₃) δ 148, 133.6, 114.8, 110.8,
103, 101.4, 71.4. HRMS calcd for C₁₄H₆F₅N, 283.0420; found,
283.0423.



4.16. 4-(4-Pentafluorophenylethynyl)iodobenzene (14). Following
the general iodination procedure via diazotization, **13** (4.3 g, 15.2
mmol) dissolved in THF (20 mL) was added to BF₃·Et₂O (7.7 mL,
60.8 mmol) followed by the addition of isoamyl nitrite (7.1 mL,
53.2 mmol). After the precipitate was isolated, it was added to a
solution of NaI (2.4 g, 16.2 mmol) and I₂ (3.1 g, 12.1 mmol) in
CH₃CN (20 mL). Purification by flash chromatography (3:1,
hexanes/CH₂Cl₂) afforded the desired product (2.1 g, 35% yield)
as a white solid; mp 121–125 °C. IR (KBr) 3016, 2621, 2485,
2434, 2216, 1918, 1713, 1498, 1438, 1367, 1223, 1113 cm⁻¹. ¹H
NMR (400 MHz, CDCl₃) δ 7.75 (m, 2H), 7.29 (m, 2H). ¹³C NMR
(100 MHz, CDCl₃) δ 137.9, 133.4, 121.1, 109.7, 99, 96.2. HRMS
calcd for C₁₄H₄F₅I, 393.9278; found, 393.9287.

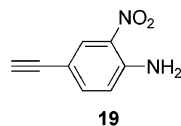


4.17. Thioacetic acid 4-(4-pentafluorophenylethynylphenylethynyl)phenyl ester (16). Following the Sonogashira coupling
protocol, **14** (520 mg, 1.4 mmol), **15**²⁵ (244 mg, 1.4 mmol), PdCl₂-
(PPh₃)₂ (93 mg, 0.14 mmol), and CuI (51 mg, 0.28 mmol) were
dissolved in THF (20 mL). TEA (0.7 mL, 5.2 mmol) was added
and the reaction was stirred at room temperature overnight.
Purification by flash chromatography (1:1, hexanes/CH₂Cl₂) af-
forded the desired product (290 mg, 47% yield) as a yellow solid;
mp 199–203 °C. IR (KBr) 3040, 2912, 2485, 2423, 2210, 1910,
1712, 1516, 1494, 1443, 1355, 1114 cm⁻¹. ¹H NMR (400 MHz,
CDCl₃) δ 7.57 (m, 6H), 7.44 (m, 2H), 2.46 (s, 3H). ¹³C NMR (100
MHz, CDCl₃) δ 193.7, 134.6, 132.6, 132.2, 132.1, 128.9, 124.6,
124.4, 121.8, 91.6, 90.7, 30.7. HRMS calcd for C₂₄H₁₁F₅OS,
442.0451; found, 442.0459.

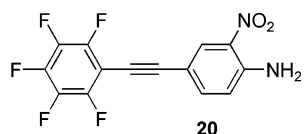


4.18. 4-(4-(4-Pentafluorophenylethynyl)phenylethynyl)benzenethiol
(**1**). Following the general deprotection of arylthioacetates, **16** (230
mg, 0.5 mmol) was dissolved in CH₂Cl₂ and MeOH (40 mL each),
with H₂SO₄ (10 drops). Flash chromatography (1:1, hexanes/CH₂-
Cl₂) afforded the desired product (98 mg, 50% yield) as a yellow
solid; mp 228–232 °C. IR (KBr) 2921, 2853, 2547, 2466, 2431,
2205, 1926, 1600, 1526, 1494, 1446, 1402, 1355, 1258, 1106 cm⁻¹.
¹H NMR (400 MHz, CDCl₃) δ 7.53 (m, 4H), 7.41 (m, 2H), 7.25

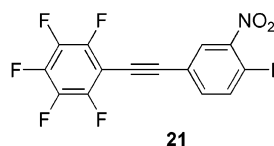
605 (m, 2H), 3.54 (s, 1H), 3.58 (s, 1H). ^{13}C NMR (100 MHz, CDCl_3)
 606 δ 136.4, 132.6, 132.4, 132, 131.7, 129.9, 129.1, 126.8, 126.5, 124.7,
 607 121.3, 120.1, 101.3, 100.3, 91.7, 89.4. HRMS calcd for $\text{C}_{22}\text{H}_9\text{F}_5\text{S}$,
 608 400.0345; found, 400.0340.



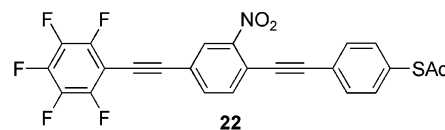
609 **4.19. 4-Ethynyl-2-nitrophenylamine (19).** Following the general
 610 deprotection of TMS-alkynes, **18**⁵⁴ (1.45 mg, 6.1 mmol) was
 611 dissolved in a mixture of CH_2Cl_2 (14 mL), MeOH (12 mL), and
 612 K_2CO_3 (3.42 g, 24.0 mmol). Flash chromatography (3:1, hexanes/
 613 CH_2Cl_2) afforded the desired product (0.9 g, 88% yield) as a bright
 614 yellow solid; mp 193–198 °C. IR (KBr) 3490, 3373, 3255, 2547,
 615 2434, 2330, 1629, 1546, 1511, 1461, 1407, 1358, 1253, 1155, 1078
 616 cm^{-1} . ^1H NMR (400 MHz, CDCl_3) δ 8.28 (d, $J = 2$ Hz, 1H), 7.43
 617 (dd $J = 8.8$, 2 Hz, 1H), 6.77 (d, $J = 8.8$ Hz, 1H), 6.26 (br s, 2H),
 618 3.01 (s, 1H). ^{13}C NMR (100 MHz, CDCl_3) δ 144.7, 138.7, 130.4,
 619 119, 110.8, 82.00. HRMS calcd for $\text{C}_8\text{H}_6\text{N}_2\text{O}_2$, 162.0429; found,
 620 162.0429.



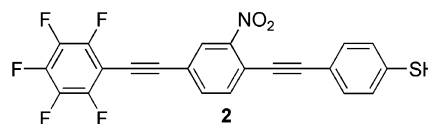
621 **4.20. 2-Nitro-4-(2,4,6-pentafluorophenylethynyl)aniline (20).** Following
 622 the Sonogashira coupling protocol, **19** (6.2 g, 38.0 mmol),
 623 bromopentafluorobenzene (19.1 g, 77.0 mmol), $\text{PdCl}_2(\text{PPh}_3)_2$ (1.0
 624 g, 4.3 mol), and CuI (0.6 g, 8.6 mmol) were dissolved in THF
 625 (100 mL). Hünig's base (27 mL, 154.0 mmol) was added and the
 626 reaction was stirred overnight at 70 °C. Purification by flash
 627 chromatography (CH_2Cl_2) afforded the desired product (3.7 g, 30%
 628 yield) as a dark yellow solid; mp 216–220 °C.; IR (KBr) 3468,
 629 3364, 3099, 2221, 1631, 1502, 1338, 1243, 1163, 1117 cm^{-1} . ^1H
 630 NMR (400 MHz, CDCl_3) δ 8.32 (s, 1H), 7.62 (d, $J = 8.8$ Hz, 1H),
 631 7.53 (br s, 2H), 7.21 (d, $J = 8.8$ Hz, 1H). ^{13}C NMR (100 MHz,
 632 CDCl_3) δ 205.7, 148.7, 138, 130.1, 120.3, 108.4, 100.8. HRMS
 633 calcd for $\text{C}_{14}\text{H}_5\text{F}_5\text{N}_2\text{O}_2$, 328.0271; found, 328.0271.



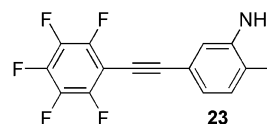
634 **4.21. 2-Iodo-5-(2,4,6-pentafluoronitrobenzene (21).** Following the
 635 general iodination procedure via diazotization, $\text{BF}_3 \cdot \text{Et}_2\text{O}$ (7.0 g,
 636 49.0 mmol) was added to a solution of **20** (1.7 g, 12.0 mmol) in
 637 THF (20 mL), followed by the addition of isoamyl nitrite (6.0 mL,
 638 43.0 mmol). After the benzenediazonium tetrafluoroborate was
 639 isolated, it was added into a solution of NaI (1.4 g, 5.0 mmol) and
 640 I_2 (1.2 g, 5.0 mmol) in CH_3CN (8 mL). Flash chromatography (2:
 641 1, hexanes/ CH_2Cl_2) gave the desired product (2.1 g, 39% yield);
 642 mp 126–128 °C. IR (KBr) 3092, 2879, 2229, 1526, 1499, 1518,
 643 1442, 1356, 1356, 1112, 1017 cm^{-1} . ^1H NMR (400 MHz, CDCl_3)
 644 δ 8.09 (d, $J = 8.4$ Hz, 1H), 8.03 (d, $J = 2$ Hz, 1H). ^{13}C NMR (100
 645 MHz, CDCl_3) δ 165.9, 142.4, 135.8, 128.3, 123.2, 117.7, 89.6, 87.8.
 646 HRMS calcd for $\text{C}_{14}\text{H}_3\text{F}_5\text{INO}_2$, 438.9128; found, 438.9120.



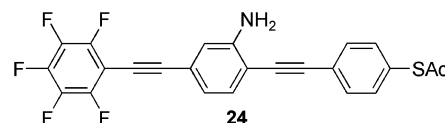
647 **4.22. Thioacetic acid 4-(2-nitro-4-(2,4,6-pentafluorophenylethynyl)-**
 648 **nylphenylethynyl)phenyl ester (22).** Following the Sonogashira
 649 coupling protocol, **21** (250 mg, 1.4 mmol), **15**²⁵ (287 mg, 1.6 mmol),
 650 $\text{PdCl}_2(\text{PPh}_3)_2$ (104 mg, 0.6 mmol), and CuI (57 mg, 1.2 mmol)
 651 were dissolved in THF (15 mL). TEA (0.7 mL, 6.0 mmol) was
 652 added and the reaction was stirred overnight at room temperature.
 653 Purification by flash chromatography (1:1, hexanes/ CH_2Cl_2) af-
 654 fforded the desired product (350 mg, 49% yield) as a yellow solid;
 655 mp 183–188 °C. IR (KBr) 3086, 2916, 2858, 2438, 2208, 1930,
 656 1698, 1606, 1530, 1493, 1442, 1348, 1266, 1121 cm^{-1} . ^1H NMR
 657 (400 MHz, CDCl_3) δ 8.29 (d, $J = 1.2$ Hz, 1H), 7.76 (m, 2H), 7.63
 658 (m, 2H), 7.45 (m, 2H), 2.46 (s, 3H). ^{13}C NMR (100 MHz, CDCl_3)
 659 δ 193.2, 135.6, 134.9, 134.4, 132.8, 130, 128.1, 123.2, 119.4, 99.1,
 660 86.1, 30.5. HRMS calcd for $\text{C}_{24}\text{H}_{10}\text{F}_5\text{NO}_3\text{S}$, 487.0301; found,
 661 487.0300.



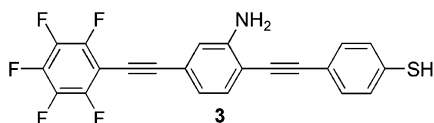
662 **4.23. 4-(2-Nitro-4-(2,4,6-pentafluorophenylethynyl)phenylethynyl)-**
 663 **benzenethiol (2).** Following the general deprotection of arylthio-
 664 acetates, **22** (255 mg, 0.5 mmol) was dissolved in CH_2Cl_2 and
 665 MeOH (5 mL each), with concentrated H_2SO_4 (5 drops). Flash
 666 chromatography (1:1, hexanes/ CH_2Cl_2) afforded the desired product
 667 (88 mg, 48% yield) as a yellow solid; mp 228–232 °C (decomp).
 668 IR (KBr) 3087, 3033, 2210, 1902, 1591, 1533, 1494, 1444, 1346,
 669 1346, 1267, 1102 cm^{-1} . ^1H NMR (400 MHz, CDCl_3) δ 8.28 (d, J
 670 $= 1.2$ Hz, 1H), 7.76 (m, 2H), 7.46 (m, 2H), 7.28 (m, 3H), 3.59 (s,
 671 1H). ^{13}C NMR (100 MHz, CDCl_3) δ 135.6, 134.7, 134.4, 132.9,
 672 128.9, 128.2, 122.1, 119.7, 119.1, 99.82, 85.3. HRMS calcd for
 673 $\text{C}_{22}\text{H}_8\text{F}_5\text{NO}_2\text{S}$, 445.0196; found, 445.0191.



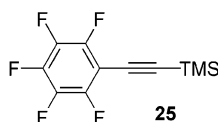
674 **4.24. 2-Iodo-5-(2,4,6-pentafluorophenylethynyl)phenylamine (23).**
 675 Into a 50-mL round-bottom flask, **21** (300 mg, 0.6 mmol) was
 676 dissolved in EtOAc (4 mL) before adding $\text{SnCl}_2 \cdot \text{H}_2\text{O}$ (617 mg, 2.7
 677 mmol). The reaction mixture was heated at reflux for 2 h, and after
 678 cooling, the mixture was dissolved in $\text{CH}_2\text{Cl}_2 \cdot \text{H}_2\text{O}$ (400 mL),
 679 followed by extractions with CH_2Cl_2 . The organic layers were
 680 combined and dried over MgSO_4 , followed by filtration and solvent
 681 removal in vacuo. Flash chromatography (2:1, hexanes/ CH_2Cl_2)
 682 afforded the desired product (175 mg, 63% yield) as a bright yellow
 683 solid; mp 158–162 °C. IR (KBr) 3452, 3367, 2920, 2222, 2178,
 684 1612, 1496, 1449, 1407, 1107 cm^{-1} . ^1H NMR (400 MHz, CDCl_3)
 685 δ 7.66 (d, $J = 8$ Hz, 1H), 6.93 (s, 1H), 6.67 (dd, $J = 8$, 1.6 Hz,
 686 1H), 4.02 (br s, 2H). ^{13}C NMR (100 MHz, CDCl_3) δ 147, 139.3,
 687 123.1, 122.6, 117.1, 86, 73.5. HRMS calcd for $\text{C}_{14}\text{H}_5\text{F}_5\text{IN}$,
 688 408.9386; found, 408.9388.



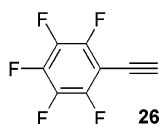
689 **4.25. Thioacetic acid 4-(2-amino-4-pentafluorophenylethynylphenylethynyl)phenyl ester (24).** Following the Sonogashira
690 coupling protocol, **23** (868 mg, 1.9 mmol), **15**²⁵ (384 mg, 2.1 mmol),
691 PdCl₂(PPh₃)₂ (139 g, 0.2 mmol), and CuI (75 mg, 0.4 mmol) were
692 dissolved in THF (15 mL). TEA (1.1 mL, 7.9 mmol) was added
693 and the reaction was left overnight at room temperature. Purification
694 by flash chromatography (1:2, hexanes/CH₂Cl₂) afforded the desired
695 product (360 mg, 38% yield) as a yellow solid; mp 216–220 °C.
696 IR (KBr) 3476, 3372, 3060, 3025, 2908, 2205, 1895, 1687, 1609,
697 1512, 1448, 1420, 1258, 1120 cm⁻¹. ¹H NMR (400 MHz, CDCl₃)
698 δ 7.58 (m, 2H), 7.39 (m, 3H), 6.97 (m, 2H), 4.21 (br s, 2H), 2.46
699 (s, 3H). ¹³C NMR (100 MHz, CDCl₃) δ 193.5, 147.8, 132.5, 132.2,
700 128.6, 124.2, 121.7, 117.3, 109.2, 96.2, 87.1, 30.5. HRMS calcd
701 for C₂₄H₁₂F₅NOS, 457.0559; found, 457.0559.



703 **4.26. 4-(2-Amino-4-pentafluorophenylethynylphenylethynyl)-**
704 **benzenethiol (3).** Following the general deprotection of arylthio-
705 acetates, **24** (165 mg, 0.3 mmol) was dissolved in CH₂Cl₂ and
706 MeOH (20 mL each) with concentrated H₂SO₄ (5 drops). Flash
707 chromatography (1:2, hexanes/CH₂Cl₂) afforded the desired product
708 (40 mg, 28% yield) as a yellow solid; mp 203–207 °C (decomp).
709 IR (KBr) 3499, 3400, 2923, 2846, 2532, 2213, 1902, 1607, 1525,
710 1492, 1259, 1107 cm⁻¹. ¹H NMR (400 MHz, CDCl₃) δ 7.40 (m,
711 2H), 7.25 (m, 2H), 6.96 (m, 3H), 4.42 (br s, 2H), 3.55 (s, 1H). ¹³C
712 NMR (100 MHz, CDCl₃) δ 150.2, 147.6, 136.4, 132.5, 129.9, 129.1,
713 126.8, 126.5, 122.4, 121.7, 120.1, 117.2, 109.6, 96.5, 85.9. HRMS
714 calcd for C₂₂H₁₀F₅NS, 415.0454; found, 415.0461.

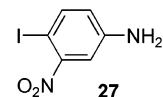


715 **4.27. Trimethylpentafluorophenylethynylsilane (25).** Follow-
716 ing the Sonogashira coupling protocol, bromopentafluorobenzene
717 (20.0 g, 81.0 mmol), PdCl₂(PPh₃)₂ (1.1 g, 1.6 mmol), and CuI (0.6
718 g, 3.2 mol) were dissolved in THF (200 mL). Hünig's base (57
719 mL, 0.3 mol) was added, followed by TMSA (23.0 mL, 162.0
720 mmol), and the mixture was stirred for 24 h at 70 °C. Purification
721 by flash chromatography (hexanes) afforded the desired product
722 (15.2 g, 71% yield) as a clear liquid. IR (neat) 3021, 2964, 2902,
723 2172, 2067, 1620, 1514, 1254, 1216, 1141 cm⁻¹. ¹H NMR (400
724 MHz, CDCl₃) δ 0.30 (s). ¹³C NMR (100 MHz, CDCl₃) δ 109.4,
725 87.4, -0.41. HRMS calcd for C₁₁H₆F₅Si, 264.0393; found,
726 264.0393.

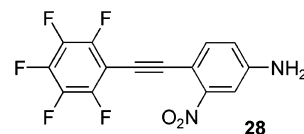


727 **4.28. 1-Ethynyl-2,3,4,5,6-pentafluorobenzene (26).** TMS-alkyne
728 **25** (39.7 g, 150.0 mmol) was dissolved in MeOH, and KOH (50%,
729 0.2 mL) was added. The exothermic reaction was stirred for 10
730 min before quenching with H₂O (200 mL) and acidifying with HCl
731 (10%, 11 mL) in order to collect a yellow precipitate. Distillation
732 (130 °C, 1 atm) gave a clear, light liquid (25 g, 87%) as the desired
733 product. IR (neat) 3313, 2955, 2778, 2640, 2467, 2436, 2129, 2041,
734 1639, 1495, 1316, 1262, 1128, 1083 cm⁻¹. ¹H NMR (400 MHz,

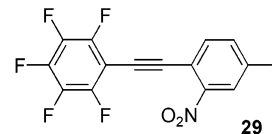
CDCl₃) δ 3.61 (s). ¹³C NMR (100 MHz, CDCl₃) δ 89.8, 67.4, 53.5. 735
HRMS calcd for C₈H₃F₅, 191.9998; found, 191.9998. 736



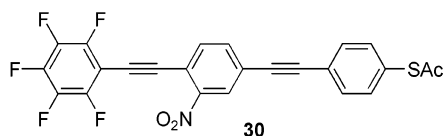
4.29. 4-Iodo-3-nitrophenylamine (27). Into a 500-mL round- 737
bottom flask, 3-nitroaniline (10.0 g, 72.4 mmol) was suspended in 738
a solution of AcOH (200 mL) and NaOAc (40.0 g, 110 mmol). 739
The reaction mixture was cooled to 0 °C and ICl (18.0 g, 110 mmol) 740
was added. The mixture was allowed to warm to room temperature 741
overnight. Saturated Na₂S₂O₃ (200 mL) was added and the mixture 742
was stirred until precipitation was observed. After filtration, the 743
orange solid was washed with water and dissolved in acetone, 744
followed by slow addition of hexanes. The precipitate was purified 745
by flash chromatography (CH₂Cl₂, then 1:1, hexanes/acetone), 746
affording the desired product (7.6 g, 41%) as a dark yellow solid; 747
mp 118–122 °C. IR (KBr) 3426, 3317, 3200, 2085, 2893, 2641, 748
1622, 1511, 1341, 1097 cm⁻¹. ¹H NMR (400 MHz, (CD₃)₂CO) δ 749
7.81 (d, *J* = 8.2 Hz, 1H), 7.52 (d, *J* = 2.4 Hz, 1H), 6.98 (dd, *J* = 750
8.2, 2.4 Hz, 1H), 5.89 (s, 2H). ¹³C NMR (100 MHz, (CD₃)₂CO) δ 751
149.8, 148.3, 139.4, 111, 106.7, 90.9. HRMS calcd for C₆H₅IN₂O₂, 752
263.9396; found, 263.9395. 753



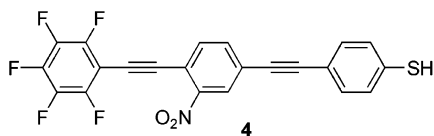
4.30. 3-Nitro-4-pentafluorophenylethynylaniline (28). Follow- 754
ing the Sonogashira coupling protocol, **27** (8.5 g, 44.0 mmol), **26**⁵⁵ 755
(11.6 g, 44.0 mmol), PdCl₂(PPh₃)₂ (620 mg, 0.8 mmol), and CuI 756
(340 mg, 1.6 mmol) were dissolved in THF (150 mL). TEA (25.0 757
mL, 177.0 mmol) was added and the reaction was stirred overnight. 758
Purification by flash chromatography (CH₂Cl₂) afforded the desired 759
product (3.4 g, 24% yield) as a dark yellow solid; mp 138–142 760
°C. IR (KBr) 3480, 3358, 2310, 2217, 1632, 1500, 1345, 1249, 761
1169, 1117 cm⁻¹. ¹H NMR (400 MHz, CDCl₃) δ 7.54 (d, *J* = 8.4 762
Hz) 7.49 (d, 1H), 7.40 (d, *J* = 2.4 Hz, 1H), 6.88 (dd, *J* = 8.4, 2.4 763
Hz, 1H), 4.27 (br s, 2H). ¹³C NMR (100 MHz, CDCl₃) δ 148.3, 764
138.8, 136.3, 126.1, 118.8, 110.1, 97.6, 93.5. HRMS calcd for 765
C₁₄H₅F₅N₂O₂, 328.0271; found, 328.0275. 766



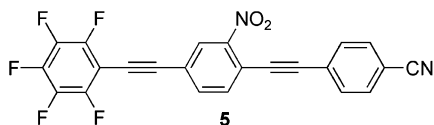
4.31. 5-Iodo-2-pentafluorophenylethynyl nitrobenzene (29). 767
Following the general iodination procedure via diazotization, **28** 768
(3.0 g, 9.1 mmol) was dissolved in CH₃CN (25 mL) and added to 769
a solution of NOBF₄ (1.7 g, 10.0 mmol) in CH₃CN (15 mL). After 770
the benzenediazonium tetrafluoroborate was isolated, it was added 771
to a solution of NaI (2.8 g, 18.2 mmol) and I₂ (3.5 g, 13.7 mmol) 772
in CH₃CN (20 mL). Flash chromatography (1:1, hexanes/CH₂Cl₂), 773
gave the desired product (3 g, 75% yield); mp 176–180 °C. IR 774
(KBr) 3083, 2217, 1625, 1519, 1436, 1340, 1276, 1110, 1031 cm⁻¹. 775
¹H NMR (400 MHz, CDCl₃) δ 8.52 (d, *J* = 1.6 Hz, 1H) 8.00 (dd, 776
J = 8.4, 1.6 Hz, 1H), 7.50 (d, *J* = 8.4 Hz, 1H). ¹³C NMR (100 777
MHz, CDCl₃) δ 149.3, 142.3, 135.9, 134, 116.7, 95.8, 94.7, 81.9. 778
HRMS calcd for C₁₄H₃F₅INO₂, 438.9128; found, 438.9129. 779



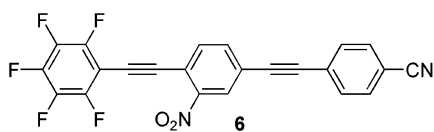
780 **4.32. Thioacetic acid 4-(3-nitro-4-pentafluorophenylethynylphenylethynyl)phenyl ester (30).** Following the Sonogashira
781 coupling protocol, **29** (500 mg, 1.1 mmol), **15**²⁵ (201 mg, 1.1 mmol),
782 PdCl₂(PPh₃)₂ (80 g, 0.1 mmol), and CuI (44 mg, 0.2 mmol) were
783 dissolved in THF (25 mL). TEA (0.7 mL, 4.5 mmol) was added
784 and the reaction was stirred at room temperature for 5 h. Purification
785 by flash chromatography (1:1, hexanes/CH₂Cl₂) afforded the desired
786 product (370 mg, 67% yield) as a yellow solid; mp 200 °C. IR
787 (KBr) 3086, 2469, 2411, 2208, 1926, 1708, 1642, 1530, 1492, 1441,
788 1354, 1227, 1122 cm⁻¹. ¹H NMR (400 MHz, CDCl₃); δ 8.31 (s,
789 1H), 7.77 (m, 2H), 7.59 (m, 2H), 7.45 (m, 2H), 2.47 (s, 3H). ¹³C
790 NMR (100 MHz, CDCl₃) δ 193.2, 135.7, 135.1, 134.5, 132.5, 129.7,
791 128, 123.1, 93.8, 88.2, 30.5. HRMS calcd for C₂₄H₁₀F₅NO₃S,
792 487.0301; found, 487.0305.



794 **4.33. 4-(3-Nitro-4-pentafluorophenylethynylphenylethynyl)-**
795 **benzenethiol (4).** Following the general deprotection of arylthio-
796 acetates, **30** (217 mg, 0.4 mmol) was dissolved in CH₂Cl₂ and
797 MeOH (20 mL each), with H₂SO₄ (10 drops). Flash chromatography
798 (1:1, hexanes/CH₂Cl₂) afforded the desired product (101 mg, 51%
799 yield) as a yellow solid; mp 228–232 °C (decomp). IR (KBr) 3083,
800 2916, 2834, 2562, 2209, 1902, 1491, 1443, 1344, 1248, 1098 cm⁻¹.
801 ¹H NMR (400 MHz, CDCl₃) δ 8.27 (m, 1H), 7.74 (m, 2H), 7.42
802 (m, 2H), 7.27 (m, 2H), 3.58 (s, 1H). ¹³C NMR (100 MHz, CDCl₃)
803 δ 135.6, 135.1, 133.9, 132.5, 129.0, 127.8, 125.9, 119, 116.2, 94.3,
804 87.2. HRMS calcd for C₂₂H₈F₅NO₂S, 445.0196; found, 445.0194.

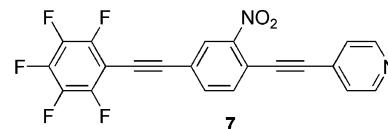


805 **4.34. 4-(2-Nitro-4-pentafluorophenylethynylphenylethynyl)-**
806 **benzonitrile (5).** Following the Sonogashira coupling protocol, **21**
807 (200 mg, 0.4 mmol), **31**¹⁴ (61 mg, 0.4 mmol), PdCl₂(PPh₃)₂ (32 g,
808 0.04 mmol), and CuI (18 mg, 0.08 mmol) were dissolved in THF
809 (15 mL). TEA (0.3 mL, 1.8 mmol) was added and the reaction
810 was left at room temperature overnight. Purification by flash
811 chromatography (1:1, hexanes/CH₂Cl₂) afforded the desired product
812 (47 mg, 23% yield) as a yellow solid; mp 238–242 °C (decomp).
813 IR (KBr) 3087, 2224, 1933, 1801, 1604, 1518, 1496, 1442, 1345,
814 1268, 1115 cm⁻¹. ¹H NMR (400 MHz, CDCl₃) δ 8.32 (d, *J* = 0.8
815 Hz, 1H), 7.77 (m, 2H), 7.7 (m, 3H), 7.64 (m, 1H). ¹³C NMR (100
816 MHz, CDCl₃) δ 135.8, 135.0, 133.2, 132.7, 132.4, 132.3, 128.2,
817 126.3, 118.6, 113.1, 97.4, 88.4. HRMS calcd for C₂₃H₇F₅N₂O₂,
818 438.0427; found, 438.0439.

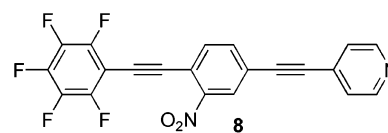


819 **4.35. 4-(3-Nitro-4-pentafluorophenylethynylphenylethynyl)-**
820 **benzonitrile (6).** Following the Sonogashira coupling protocol, **29**

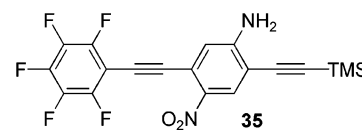
(200 mg, 0.4 mmol), **31**¹⁴ (61 mg, 0.4 mmol), PdCl₂(PPh₃)₂ (32
821 mg, 0.04 mmol), and CuI (18 mg, 0.08 mmol) were dissolved in
822 THF (15 mL). TEA (0.3 mL, 1.8 mmol) was added and the reaction
823 was stirred at room temperature overnight. Purification by flash
824 chromatography (1:1, hexanes/CH₂Cl₂) afforded the desired product
825 (90 mg, 46% yield) as a yellow solid; mp 210–214 °C (decomp).
826 IR (KBr) 3090, 2223, 1922, 1606, 1530, 1497, 1443, 1399, 1345,
827 1269, 1113 cm⁻¹. ¹H NMR (400 MHz, CDCl₃) δ 8.47 (d, *J* = 2.4
828 Hz, 1H), 8.24 (dd, *J* = 8.4, 2.4 Hz 1H), 7.81 (d, *J* = 8.4, 1H), 7.70
829 (m, 4H). ¹³C NMR (100 MHz, CDCl₃) δ 147.8, 133.6, 133.2, 132.6,
830 132.4, 132.3, 130.2, 127.4, 126.6, 126.3, 123.5, 118.4, 113.1, 99.7,
831 94.5, 89.2, 81.6. HRMS calcd for C₂₃H₇F₅N₂O₂, 438.0427; found,
832 438.0417. 833



834 **4.36. 4-(2-Nitro-4-pentafluorophenylethynylphenylethynyl)-**
835 **pyridine (7).** Following the Sonogashira coupling protocol, **21** (230
836 mg, 0.52 mmol), **32**²⁸ (70 mg, 0.68 mmol), PdCl₂(PPh₃)₂ (25 mg,
837 0.03 mmol), and CuI (18 mg, 0.09 mmol) were dissolved in THF
838 (30 mL). TEA (15 mL) was added and the mixture was stirred at
839 65 °C for 16 h. Purification by flash chromatography (4:1, CH₂-
840 Cl₂/Et₂O) afforded the desired product (120 mg, 55% yield) as a
841 yellow fluffy solid; mp 175–179 °C. IR (KBr) 3431, 3089, 2227,
842 1589, 1547, 1521, 1498, 1444, 1408, 1346, 1260, 1215, 1120 cm⁻¹.
843 ¹H NMR (400 MHz, CDCl₃) δ 8.68 (br s, 2H), 8.31 (d, *J* = 1.5
844 Hz, 1H), 7.81 (dd, *J* = 8.1, 1.5 Hz, 1H), 7.76 (d, *J* = 8.1 Hz, 1H),
845 7.45 (d, *J* = 5.7 Hz, 2H). ¹³C NMR (100 MHz, CDCl₃) δ 150.2,
846 149.9, 135.8, 135.2, 130.3, 128.2, 125.8, 123.4, 118.5, 97.1, 96.3,
847 88.4. HRMS calcd for C₂₁H₇F₅N₂O₂, 414.0427; found, 414.0467.
848 Anal. Calcd: C, 60.88; H, 1.70; N, 6.76. Found: C, 60.81; H, 1.59;
849 N, 6.72.

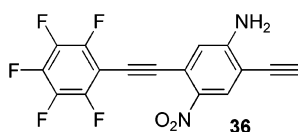


850 **4.37. 4-(3-Nitro-4-pentafluorophenylethynylphenylethynyl)-**
851 **pyridine (8).** Following the Sonogashira coupling protocol, **29** (322
852 mg, 0.73 mmol), **32**²⁸ (91 mg, 0.88 mmol), PdCl₂(PPh₃)₂ (26 mg,
853 0.08 mmol), and CuI (14 mg, 0.16 mmol) were dissolved in THF
854 (20 mL). TEA (15 mL) was added and the mixture was stirred at
855 60 °C for 2 d. Purification by flash chromatography (4:1, CH₂Cl₂/
856 Et₂O) afforded the desired product (78 mg, 26% yield) as a yellow
857 fluffy solid; mp 175–179 °C. IR (KBr) 3094, 2223, 1645, 1590,
858 1542, 1522, 1498, 1446, 1407, 1348, 1248 cm⁻¹. ¹H NMR (400
859 MHz, CDCl₃) δ 8.68 (br s, 2H), 8.34 (t, *J* = 1.1 Hz, 1H), 7.80 (m,
860 2H), 7.42 (m, 2H). ¹³C NMR (100 MHz, CDCl₃) δ 150.3, 149.5,
861 135.9, 135.3, 130.2, 128.3, 125.7, 124.7, 117.4, 91.4, 90.6, 82.6.
862 HRMS calcd for C₂₁H₇N₂O₂, 414.0427; found, 414.0427.



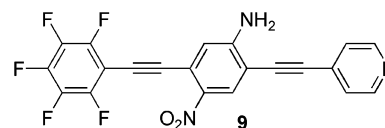
863 **4.38. 4-Nitro-5-pentafluorophenylethynyl-2-trimethylsilyl-**
864 **phenylamine (35).** Following the Sonogashira coupling
865 protocol, **33** (3.8 g, 13.0 mmol), **26** (2.5 g, 13.0 mmol), PdCl₂-
866 (PPh₃)₂ (370 mg, 0.1 mmol), and CuI (200 mg, 0.2 mmol) were
867 dissolved in THF (150 mL). TEA (7.2 mL, 57.0 mmol) was added

868 and the mixture was stirred at 60 °C for 2 d. Purification by flash
 869 chromatography (CH₂Cl₂) afforded an inseparable mixture of mono-
 870 adduct and bis-adduct according to HRMS. The bright yellow solid
 871 was taken immediately to the next step with no further clean
 872 characterization of the mono-adduct. Under the same Sonogashira
 873 coupling protocol, the same amounts of PdCl₂(PPh₃)₂, CuI, and TEA
 874 were added and dissolved in THF (100 mL). Excess TMSA (5.0
 875 mL, 35.0 mmol) was added and the reaction mixture was stirred at
 876 60 °C for 2 d. Purification by flash chromatography (2:1, hexanes/
 877 CH₂Cl₂) afforded the desired product **35** (1.4 g, 26% yield over
 878 two steps) as a yellow fluffy solid; mp 143–147 °C (decomp). IR
 879 (KBr) 3094, 2223, 1645, 1590, 1542, 1522, 1498, 1446, 1407, 1348,
 880 1248 cm⁻¹. ¹H NMR (400 MHz, CDCl₃) δ 8.19 (s, 1H), 7.18 (s,
 881 1H), 5.51 (br s, 2H), 0.32 (s, 9H). ¹³C NMR (100 MHz, CDCl₃) δ
 882 153.9, 137.8, 131.0, 130.6, 119.0, 118.7, 107.4, 103.7, 99.0, 98.2,
 883 79.4, -0.5. HRMS calcd for C₁₉H₁₃F₅N₂O₂Si, 424.066; found,
 884 424.0658.



885 **4.39. 2-Ethynyl-4-nitro-5-pentafluorophenylethynylphenyl-**
 886 **amine (36).** Following the general deprotection of TMS-alkynes,
 887 **35** (980 mg, 0.23 mmol) was dissolved in MeOH (20 mL), and
 888 K₂CO₃ (100 mg 0.7 mmol) was added. Purification by flash
 889 chromatography (CH₂Cl₂) gave the desired product (750 mg, 93%)
 890 as a light yellow solid; mp 243–247 °C (decomp). IR (KBr) 3313,
 891 2955, 2778, 2640, 2467, 2436, 2129, 2041, 1639, 1495, 1316, 1262,
 892 1128, 1083 cm⁻¹. ¹H NMR (400 MHz, CDCl₃) δ 8.21 (s, 1H),
 893 7.17 (s, 1H), 6.45 (br s, 2H), 4.25 (s, 1H). ¹³C NMR (100 MHz,
 894 CDCl₃) δ 154.3, 130.8, 118.7, 106.5, 87.2, 77.9. HRMS calcd for
 895 C₁₆H₅F₅N₂O₂, 352.0271; found, 352.0253.

896 **4.40. 4-Nitro-5-pentafluorophenylethynyl-2-pyridin-4-ylethy-**
 897 **nylphenylamine (9).** Following the Sonogashira coupling protocol,
 898 **36** (365 mg, 1.0 mmol), **37**¹⁵ (255 mg, 1.2 mmol), PdCl₂(PPh₃)₂
 899 (36 mg, 0.01 mmol), and CuI (20 mg, 0.02 mmol) were dissolved



900 in THF (40 mL). TEA (20 mL) was added and the mixture was
 901 stirred at 60 °C for 24 h. Purification by flash chromatography
 902 (EtOAc) afforded the desired product (206 mg, 46% yield) as a
 903 yellow powder; mp slow decomp. IR (KBr) 3442, 3300, 3134, 2212,
 904 1641, 1596, 1546, 1520, 1496, 1318 cm⁻¹. ¹H NMR (400 MHz,
 905 THF-*d*₈) δ 8.60 (br s, 2H), 8.31 (s, 1H), 7.48 (d, *J* = 5.2 Hz, 2H),
 906 6.99 (s, 1H), 6.41 (br s, 2H). ¹³C NMR (500 MHz, THF-*d*₈) δ 154.6,
 907 151.1, 138.5, 138.2, 131.7, 131.6, 131.1, 128.0, 126.2, 120.2, 119.6,
 908 107.0, 99.2, 95.1, 88.5. HRMS calcd for C₂₁H₈F₅N₃O₂, 429.0537;
 909 found, 429.0531.

910 **Acknowledgment.** This work was funded by the Defense
 911 Advanced Research Projects Agency, the Office of Naval
 912 Research, and the National Institute of Standards and Testing
 913 (U.S. Department of Commerce). We are grateful to R. Stanley
 914 Williams and Zhiyong Li of Hewlett-Packard Laboratories QSR,
 915 Palo Alto, CA for providing materials and equipment necessary
 916 to obtain the FTIR spectrum in Figure 10. We thank Dr. I
 917 Chester of FAR Research Inc. for providing trimethylsilylacety-
 918 lene, and Prof. Jorge Seminario for helpful advice with the DFT
 919 calculations.

920 **Supporting Information Available:** Material and general
 921 procedures, general procedure for coupling of terminal alkynes with
 922 aryl halides (Castro-Stephens/Sonogashira protocol), general pro-
 923 cedure for alkaline deprotection of TMS-protected alkynes, general
 924 procedure for iodination of anilines via diazotization, and general
 925 procedure for acid-deprotection of arylthioacetates (pdf). This
 926 material is available free of charge via the Internet at
 927 <http://pubs.acs.org>.

CM0486161

928